[bioRxiv]

Stimulatory and inhibitory G-protein signaling relays drive cAMP accumulation for timely metamorphosis in the chordate *Ciona*

Akiko Hozumi[1,7], Nozomu M. Totsuka[2,6], Arata Onodera[1], Yanbin Wang[1], Mayuko Hamada[3], Akira Shiraishi[4], Honoo Satake[4], Takeo Horie[5], Kohji Hotta[2], Yasunori Sasakura[1,7,*]

1 Shimoda Marine Research Center, University of Tsukuba
2 Department of Biosciences and Informatics, Faculty of Science and Technology, Keio University
3 Ushimado Marine Institute, Okayama University
4 Bioorganic Research Institute, Suntory Foundation for Life Sciences
5 Laboratory for single-cell Neurobiology, Graduate School of Frontier Biosciences, Osaka University
6 These authors contributed equally
7 Lead contact

*Correspondence: sasakura@shimoda.tsukuba.ac.jp

48 pages of manuscript with references and Figure legends; 7 Figures; 6 Supplementary Figures; 2 Supplementary Tables.

Abstract

Larvae of the ascidian *Ciona* initiate metamorphosis tens of minutes after adhesion to a substratum via its adhesive organ. The gap between adhesion and metamorphosis initiation is suggested to ensure the rigidity of adhesion, allowing *Ciona* to maintain settlement after losing locomotive activity through metamorphosis. The mechanism producing the gap is unknown. Here, by combining gene functional analyses, pharmacological analyses, and live imaging, we propose that the gap represents the time required for sufficient cAMP accumulation to trigger metamorphosis. Not only the Gs pathway but also the Gi and Gq pathways are involved in the initiation of metamorphosis in the downstream signaling cascade of the neurotransmitter GABA, the known initiator of *Ciona* metamorphosis. The mutual crosstalk of stimulatory and inhibitory G-proteins functions as the accelerator and brake for cAMP production, ensuring the faithful initiation of metamorphosis at an appropriate time and in the right situation.

Introduction

Metamorphosis is a widespread feature of animal development that allows them to have different functions between larval and adult stages [1]. As larvae become adults, the shape and various characteristics of their physiology, gene expression, behavior, and lifestyle change. With these changes, animals can focus on a limited number of biological activities at each stage to increase feeding, growth, dispersal, and reproduction efficiencies. This biphasic mode of life is a widely conserved and ancient trait of animals, as evidenced by its presence in groups that maintain primitive states [2], indicating that this long-conserved feature has contributed to animals' flourishment. Therefore, to understand animal evolution, it is essential to elucidate the mechanisms underlying metamorphosis.

A key characteristic of metamorphosis is that both internal and external conditions determine its initiation. Sufficiently matured (or metamorphically competent[3]) larvae start metamorphosis only when they meet an appropriate external condition to be adults. Various organic and inorganic external stimuli suited to the lifestyle of adulthood trigger metamorphosis. Many marine invertebrates exhibit a benthic lifestyle at the adult stage[4]. Their planktonic larvae have an adhesive organ that secretes adhesives and triggers metamorphosis when they adhere to a substratum. Upon starting metamorphosis, their larvae lose locomotive organs and transition into benthic adult forms. Determining the timing of metamorphosis is important for benthic animals, particularly sessile ones, to ensure their future survival and reproduction, as they become unable to move after metamorphosis. Therefore, sessile animals are suspected to have elaborate mechanisms to start metamorphosis only when a firm adhesion is achieved at an appropriate place. Although several reports describe this kind of

phenomenon[5–7], the mechanism by which the external condition is turned into an internal mechanism to trigger metamorphosis at the right timing remains elusive.

Ascidians are marine invertebrate chordates that are the closest living relatives to vertebrates[8,9]. The chordate features of ascidians are best represented by their tadpole larval shape. Like vertebrate tadpoles, ascidian larvae swim by beating their tail through neuromuscular activities[10,11]. However, ascidians lose the tadpole shape during metamorphosis, and they exhibit a sessile lifestyle at the adult stage[12,13]. Ascidian metamorphosis comprises several key events, such as tail regression, body axis rotation, and adult organ growth[14] (Figure 1A).

Adhesion to a substratum triggers ascidian metamorphosis[14]. Ascidian larvae have adhesive organs called adhesive papillae, usually triangular protrusions at the anterior end. Adhesive papillae secrete a lectin-type mucus substance that is suspected to aid in binding to the substratum[15]. Moreover, adhesive papillae serve as mechanical sensors[16]. The papilla is a neuronal organ that includes epidermal neurons positive for vesicular glutamate transporter (vGLUT) and GABA, which innervate axons toward the sensory vesicle (larval brain)[17–20]. The papilla neurons are responsible for initiating metamorphosis[16,21–23]. Moreover, our recent study suggests the involvement of a mechanoreceptor channel (the TRP channel) in the responsiveness to mechanical stimuli[22]. However, a simple physical adhesion is not sufficient to trigger metamorphosis. In our study using the model ascidian *Ciona intestinalis* Type A (this species has been suggested to be renamed *C. robusta* [24–26], and hereafter we call it *Ciona*), continuous adhesion for about 30 min is necessary before starting metamorphosis[27]. When larvae detach before reaching the critical period, they must adhere for 30 min again for metamorphosis. Therefore, ascidian larvae are suspected of

sensing the duration of adhesion and initiating metamorphosis only when adhesion is firm enough to be maintained for the required period. *Ciona* larvae continue tail beating during adhesion to push their body to the substratum. We showed that the strength of force generated by this swimming activity influences the timing of metamorphosis initiation[22]. In this phenomenon, abolishment of swimming activity elongates the time from settlement until metamorphosis is initiated. The mechanisms for measuring the duration of adhesion and the strength of the force generated by adhesion are unknown.

To elucidate the mechanisms triggering ascidian metamorphosis, the signaling pathways must be characterized. Many studies have discovered signaling molecules as possible inducers of ascidian metamorphosis[28–35]. These molecules include neurotransmitters, suggesting that transmission of excitation in the nervous system, starting from the adhesive papillae, is crucial for metamorphosis. Recently, our group reported that the inhibitory neurotransmitter GABA plays a pivotal role in initiating *Ciona* metamorphosis[36]. Knockout and knockdown of the genes encoding GABA synthase (GAD), vesicular inhibitory amino acid transporter (VIAAT or VGAT), and metabotropic GABA receptor (GABABR) resulted in the perturbation of metamorphosis. Moreover, GABA administration induces metamorphosis without adhesion. Our previous studies demonstrated that GABA induces the secretion of gonadotropin-releasing hormone (GnRH)[36,37]; however, it remains unknown how the inhibitory neurotransmitter activates neuronal functions for initiating metamorphosis.

In this study, we addressed the characterization of the downstream cascade stimulated by GABA. Because GABABR is a G-protein-coupled receptor (GPCR)[38], we searched for trimeric G-proteins necessary for metamorphosis. These G-proteins are heterotrimers of an α β and γ subunit[39]. Upon ligand binding, GPCR exchanges GDP of

the α subunit to GTP, then the GTP-bound α subunit and the βγ complex are released from the GPCR. Although both the GTP-bound α subunit and the βγ complex have activities, the α subunit mainly determines the reaction specific to the G-protein type. We found that three G-proteins are activated in the downstream GABA cascade, resulting in cyclic adenosine monophosphate (cAMP) elevation. Because the signaling includes stimulating and inhibiting cAMP synthesis, *Ciona* initiates metamorphosis only when a sufficient quantity of cAMP is accumulated due to sustained adhesion. Our results revealed the ingenious mechanism that permits *Ciona* to start metamorphosis only when achieving an appropriate adhesion firm enough to relinquish swimming ability and commence sessile adult life.

Results

Characterization of G-proteins necessary for metamorphosis initiation

We knocked down the genes encoding G alpha (Gα) proteins[40] using antisense morpholino oligonucleotides (MOs). We found that two genes corresponding to Gαq and Gαs are necessary for metamorphosis. Neither morphant showed any signature of metamorphosis even though both were allowed to adhere to the base of culture dishes, which was sufficient for control larvae to initiate metamorphosis (Figure 1A-F).

Gαq activates phospholipase C beta (PLCβ) to produce inositol triphosphate (IP3)[41]. IP3 is received by its receptor on the endoplasmic reticulum (ER) and releases calcium ion (Ca^{2+}). The *Ciona* genome encodes two PLCβ (PLCβ1/2/3, PLCβ4) and one IP3 receptor (IP3R) (Figure S1 and Table S1). We knocked down *PLCβ1/2/3*, *PLCβ4*, and *IP3R* genes. The knockdown larvae of these three genes failed to start

metamorphosis (Figure 1G-I), suggesting that Gαq initiates metamorphosis by the conventional Ca^{2+} pathway mediated by PLCβ and IP3/IP3R. To confirm this, we overexpressed a constitutively active form of Gαq (caGαq)[42] and of caPLCβ1/2/3[43] in the entire nervous system with the *cis* element of the gene encoding prohormone convertase 2 (PC2)[44–46]. When the microinjected animals reached the larval stage, they were cultured on agar-coated dishes after tail amputation to prevent adhesion. In this condition, the control larvae rarely started metamorphosis because of the absence of adhesion (Figure 1J). In contrast, ca*Gαq*- or ca*PLCβ1/2/3*-overexpressed larvae initiated metamorphosis without adhesion (Figure 1K-M).

Adhesive papillae exhibit a Ca^{2+} increase soon after sensing an adhesive stimulus[16,22]. We examined whether this Ca^{2+} transient is dependent on the Gq pathway. Compared to controls, significantly fewer larvae injected with *Gαq* MO plus *GCaMP8* mRNA exhibited GCaMP8 fluorescence elevation in the adhesive papilla upon stimulation (Figure 1N, O). This result suggests that the Gq pathway is activated upon adhesion to cause a Ca^{2+} transient in the adhesive papilla.

Gs pathway initiates metamorphosis by activating cAMP synthesis

The involvement of Gs in metamorphosis was confirmed by the overexpression of a constitutively active form of Gαs (caGαs)[47] in the nervous system. This overexpression resulted in the initiation of metamorphosis without adhesion (Figure 2A-C). The Gs pathway activates adenylate cyclase (AC) to produce cAMP[48]. We previously reported that cAMP can induce metamorphosis[37]. Because externally added cAMP is not a strong inducer of metamorphosis, we attempted to confirm this hypothesis through another experiment. Theophylline increases cAMP by inhibiting the cAMP-degrading enzyme

phosphodiesterase (PDE)[49]. We treated wild-type larvae with theophylline after tail amputation to prevent larvae from adhesion. Most theophylline-treated larvae completed tail regression without adhesion (Figure 2D-F). Theophylline has several target proteins in addition to PDE[50]. To further confirm that cAMP is responsible for the initiation of metamorphosis, we overexpressed photo-activating AC (bPAC)[51] in the nervous system. The *bPAC*-overexpressed larvae regressed their tails without adhesion, suggesting that a cAMP increase triggers metamorphosis (Figure 2G).

Using bPAC, we addressed whether enhanced cAMP production facilitates the initiation of metamorphosis. At 24 hours post-fertilization (hpf), only a few animals in both the *bPAC*-overexpressed and control groups initiated metamorphosis because 24 hpf is somewhat too early for *Ciona* larvae to be metamorphically competent[27] (Figure 2H). Even in this condition, the *bPAC*-overexpressed group exhibited a statistically higher rate of metamorphosis-initiated larvae. The proportion of animals initiating metamorphosis increased over successive time points, with the *bPAC*-overexpressed group consistently showing a statistically higher rate of metamorphosis compared to controls. These results support the idea that cAMP plays a role as a timer for *Ciona* metamorphosis; accumulation of this molecule to exceed a threshold could trigger metamorphosis. Because many of the *bPAC*-overexpressed larvae did not initiate metamorphosis at 24 hpf, similar to control larvae, cAMP accumulation does not alter the timing of acquiring metamorphic competence.

Gq-Gs pathways work in the adhesive papillae for metamorphosis

The above results showed that activation of the Gq and Gs pathways are the key events in initiating metamorphosis. Gαq is necessary to induce Ca^{2+} transients in the adhesive

papillae, suggesting that the Gq pathway functions in this region. If both Gq and Gs function in the papillae, they should be expressed in the adhesive papilla. The transcriptome analysis of the larval papilla region showed that the genes encoding Gq and Gs pathway proteins are expressed in this region (Figure S2 and Table S1). Therefore, Gq and Gs could function in the papilla to initiate metamorphosis.

As shown above, theophylline induced metamorphosis without settlement. However, when papillae were removed from larvae, theophylline failed to induce metamorphosis (Figure 3A-C). This suggests that cAMP elevation in the adhesive papillae is essential for starting metamorphosis. The overexpression of *caGαq*, *caPLCβ1/2/3*, *caGαs*, and *bPAC* by the *PC2 cis* element resulted in the initiation of metamorphosis without adhesion. Like theophylline, amputation of the papillae inhibited them from starting metamorphosis (Figure 3D), confirming that activation of the Gq and Gs pathways in the adhesive papillae triggers metamorphosis.

If the Gs pathway is activated in the adhesive papillae, a cAMP increase should be observed in this region upon adhesion. We examined this possibility using a fluorescent cAMP indicator called Pink Flamindo (PF)[52]. After stimulation, the fluorescence of PF in the papillae temporarily decreased on average by 0.83-fold (n=5) from the initial intensity, followed by a gradual increase to 1.17-fold over successive time points (Figure 3E). Such an increase in fluorescence intensity was not observed in the adhesive papillae of the larvae that had failed to initiate metamorphosis following stimulation (n=4, Figure S3). Therefore, increased cAMP in the papillae serves to indicate that sufficient stimuli of adhesion have been received to induce metamorphosis. This strengthens our hypothesis that cAMP accumulation in the adhesive papillae determines the initiation of metamorphosis.

GABA in the adhesive papillae is responsible for metamorphosis

Our previous study demonstrated that GABA is the chief neurotransmitter that induces metamorphosis[36]. To gain insight into the relationships between the GABA, Gq, and Gs pathways, we addressed whether GABA functions in the adhesive papillae for initiating metamorphosis, similar to Gq and Gs.

The previous studies and our transcriptome data suggest that GAD is expressed in the adhesive papillae[53] (Table S1). Moreover, GABA-immunopositive signals have been detected in the papillae[19,53]. Therefore, papillae can provide GABA to stimulate themselves. Next, we examined whether the adhesive papillae can receive GABA to initiate metamorphosis. We showed that the metabotropic GABA receptor is responsible for the initiation of metamorphosis[36]. Using whole-mount *in situ* hybridization, the previous study did not detect the expression of two GABAB receptor (GABABR) genes in the papillae[53]; however, our transcriptome data detected the low-level expression of three genes encoding GABABR (Table S1) in the papillae, suggesting that adhesive papillae could receive GABA. GABA can induce metamorphosis without adhesion (Figure S4A)[36]. However, amputation of adhesive papillae eliminated this activity (Figure S4B-C), suggesting that GABA reception by the papillae is responsible for starting metamorphosis.

The larval brain is the major domain expressing *GABABR*[53]. Therefore, it remains possible that GABA signaling in the brain stimulates the papillae in a retrograde manner to initiate metamorphosis. The connectome analyses of the larval nervous system did not suggest a nerve that inputs into the papillae from the brain[54,55]; however, retrograde stimulation would be possible through the volume transmission of a

signaling molecule. To examine this possibility, we isolated larval fragments anterior to the brain (Figure S4D), followed by the administration of GABA and theophylline. Through the application of these chemicals, anterior fragments exhibited increased clarity, elongation, and retraction of papillae, which are the signatures of metamorphosis (Figure S4E-G). Because their responses to GABA were weaker than those observed in the theophylline treatment, we further examined whether the anterior fragments can respond to GABA by monitoring the expression of GABA-responsive genes. By comparing expression levels between control and GABA-administered larvae, we made a list of the genes upregulated by GABA in the papillae (Table S2). Among them, we compared the expression levels of two genes (KY21.Chr5.240 and KY21.Chr8.489) between GABA-administered and control anterior fragments. GABA-treated anterior fragments expressed these genes at levels at least three times higher than controls (Figure S4H). We concluded that GABA is secreted from and stimulates the papillae to start metamorphosis.

Gs/cAMP is downstream of the Gq pathway

Our next question is: What are the upstream or downstream relationships between GABA, Gq/Ca2+, and Gs/cAMP in the adhesive papillae? We first examined the relationships between the Gq and Gs pathways. Theophylline ameliorated metamorphosis-failed phenotypes in *Gαq*, *PLCβ*, and *IP3R* knockdowns (Figure 4A-E). Moreover, *Gαq* morphants initiated metamorphosis when ca*Gαs* was overexpressed in the nervous system (Figure 4F). These results suggest that the Gq pathway is upstream of the Gs/cAMP pathway. *Gαs* knockdown larvae exhibited Ca^{2+} transients in the adhesive papillae upon stimulation (Figure 4G). Because this Ca^{2+} transient is Gq-

dependent (Figure 1O), this result confirms that the Gs pathway is downstream of the Gq-dependent Ca^{2+} increase.

To gain further insight into the epistatic order of the Gq and Gs pathways, we overexpressed constitutive active forms of Gq pathway proteins in *Gαs* morphants with the *PC2 cis* element. If Gq is upstream of the Gs pathway, forced activation of the Gq pathway by caGαq or caPLCβ1/2/3 would not ameliorate the *Gαs* MO effect. Indeed, ca*PLCβ1/2/3*, which rescued *Gαq* morphants well, failed to rescue *Gαs* morphants (Figure 4H-L). In contrast, ca*Gαq* significantly ameliorated the metamorphosis-failed phenocopies of *Gαs* morphants (Figure 4M), contradicting the hypothesis that Gq is upstream of the Gs pathway. One possibility is that the Gq pathway stimulates cAMP synthesis through a massive Ca^{2+} increase and protein kinase C (PKC) activation[56,57]. Indeed, *Ciona* larvae can synthesize cAMP without Gs, as suggested by the partial rescue of *Gαs* morphants by theophylline treatment (Figure 4N). These data suggest that Gαs-independent AC could be a target of the Gq pathway. We concluded that the Gq pathway is upstream of the Gs pathway in the signaling cascade initiating *Ciona* metamorphosis.

Interaction between GABA and Gq pathways

We next investigated the relationships between the GABA and Gq/Gs pathways. As our previous study showed, GABA pathway knockdown by *GAD* or *GABABR1* MO disrupted the initiation of metamorphosis (Figure 5A)[36]. Overexpression of ca*PLCβ1/2/3* and theophylline treatment ameliorated the metamorphosis-failed phenocopies of *GAD*/*GABABR1* morphants (Figure 5B-D). These results suggest that the GABA pathway is upstream of the Gq and Gs pathways. We observed Ca^{2+}

transients in the adhesive papillae of *GAD* knockdown larvae. *GAD* morphants rarely exhibited a Ca^{2+} increase after stimulation (Figure 5E). Because the Ca^{2+} transient in the papillae is Gq-dependent, this result confirms that the GABA pathway is upstream of, or at least in parallel with, the Gq pathway.

However, puzzling results were obtained when we administered *Gαq*- and *Gαs*-knockdown larvae with GABA. If GABA is upstream of the Gq and Gs pathways, this chemical does not induce metamorphosis when the Gq or Gs pathway is disrupted. However, GABA significantly ameliorated the metamorphosis-failed phenocopies of *Gαq*, *PLCβ*, and *Gαs* morphants (Figure 5F-H). These results could be explained by assuming enhancement of the Gq pathway by GABA through PLCβ and another GABA-mediated metamorphic pathway bypassing Gq components. These possibilities are examined in the next section.

Contribution of Gi to metamorphosis

The function of GABA as the potential upstream factor of Gq could be easily explained if GABABR is coupled with Gq. Although a few studies suggest this possibility[58], Gi is regarded as the major G-protein coupled with GABABR[59]. A previous study suggested that the *Ciona* genome encodes one typical Gαi protein[40]. The gene encoding this Gαi is strongly expressed in the entire larval nervous system including adhesive papillae[60]. The knockdown of this gene exhibited a significantly reduced rate of metamorphosis (Figure 6A); however, the reduction was not conspicuous, suggesting the presence of another Gαi regulating metamorphosis.

A previous study showed that *Ciona* has four *Ciona*-specific Gα proteins[40]. We found three gene models (KY21.Chr2.875, KY21.Chr4.943, and KY21.Chr9.455)

encoding these divergent Gα proteins from the newest genome database[61]. Our phylogenetic analyses showed that the divergent Gα proteins have a strong affinity to the Gαi/o family proteins (Figure S5A). Moreover, the amino acid residues at the C-terminal end of KY21.Chr2.875 are more similar to human Gαi than the other Gα proteins (Figure S5B). The C-terminal residues, particularly glycine at position 3, are essential for determining the G-protein partner of GPCR[62]. We tentatively name this protein dvGαi_Chr2. The transcriptome data showed that the gene encoding dvGαi_Chr2 is strongly expressed in the papillae (Table S1). The *dvGαi_Chr2* knockdown larvae failed to initiate metamorphosis (Figure 6B-C), and this phenocopy was rescued by theophylline and GABA (Figure 6D-E), suggesting that *dvGαi_Chr2* is necessary for metamorphosis. This strengthens the hypothesis that GABABR regulates metamorphosis through Gi. The rescue of *dvGαi_Chr2* morphants by GABA could be attributable to a redundant function of the typical Gαi protein in the papillae.

We further explored the involvement of Gi upon metamorphosis as the upstream factor of the Gq-Gs pathways. Gi is known to activate PLCβ through the Gβγi complex[63,64]. Released βγ is inactivated by overexpressing normal (usually GDP-bound) Gα subunits because GDP-Gα quenches the βγ complex[65]. Overexpressing wild-type *Gαi* and *Gαs* in the nervous system suppressed metamorphosis (Figure 6F), suggesting that the activated βγ complex is necessary for initiating metamorphosis. To confirm that the wild-type Gαi exerts its effect through the sequestration of the βγ complex, we overexpressed a dominant-negative form of Gαi (dnGαi)[66,67] which has reduced GDP/GTP affinity while maintaining βγ binding activity. dnGαi significantly reduced the occurrence of metamorphosis (Figure 6G), suggesting that the negative effect of Gαi on metamorphosis occurs through interaction with the βγ complex.

If Gβγ-mediated PLCβ activation is used in *Ciona* metamorphosis, PLCβ receives two independent inputs (Gαq and Gβγi) for its activation. These pathways could compensate for each other. We noticed that the MOs for GABA pathway genes and the *Gαq* MO did not strongly disrupt metamorphosis compared to the *Gαs* MO (Figure 1E-F; 5C-D). The compensatory role could explain this phenomenon. Indeed, the simultaneous knockdown of *GABABR1* and *Gαq* resulted in a strong impairment of metamorphosis (Figure 6H), and these morphants initiated metamorphosis by overexpression of ca*PLCβ1/2/3* or ca*Gαs* (Figure 6I).

If the role of the GABA/Gi pathway relies specifically on PLCβ activation in the mechanism of metamorphosis, GABA administration would not rescue *PLCβ* morphants. However, GABA weakly but significantly induced metamorphosis in *PLCβ1/2/3* plus *PLCβ4* double-knockdown larvae (Figure 5G). Therefore, GABA/Gi is likely to activate another pathway that bypasses PLCβ. Gβγi is known to activate group III AC[56]. Its *Ciona* counterpart (AC5/6) is expressed in the adhesive papillae (Figure S2B), which could explain the results of the rescue experiments. In addition, there are two other major targets of Gβγi. One is the G-protein-activated inwardly rectifying potassium (GIRK) channel[68]. Our RNA-seq data on the papillae indicated the expression of two GIRK channel genes (Table S1). The GIRK channel negatively regulates the excitation of neurons through hyperpolarization. If the metamorphosis of *Ciona* is induced by the excitation of papilla neurons as suggested previously[16,22], the GIRK channel is likely to regulate metamorphosis negatively. Indeed, the knockdown of one GIRK channel gene weakly enhanced the initiation of metamorphosis without settlement (Figure 6J). Although the negative role of the GIRK channel supports the involvement of Gβγi in the pathway of metamorphosis, this does not explain the PLCβ-

independent activation of the metamorphic pathway by GABA/Gi.

The third function of Gβγi is to activate MAPK signaling through positive regulation of MEK[69]. PLCβ does not mediate this pathway. It has been suggested that MAPK signaling is required to induce metamorphosis[70,71]. To show that MEK activation is necessary for inducing metamorphosis mediated by GABA, we treated adhesion-prevented larvae with GABA plus U0126, a potent MEK1/2 inhibitor repeatedly used in ascidians[72,73]. U0126 reduced the rate of metamorphosis induction by GABA (Figure 6K).

cAMP is also known to activate the pathway that involves MEK1/2[74]. We found that U0126 antagonized the effect of theophylline on metamorphosis (Figure 6L). Therefore, GABA and cAMP have the same target (MEK1/2) to initiate metamorphosis, suggesting their compensatory function and/or that cAMP synthesis is upregulated by GABA-Gβγi. These bypassing pathways could explain the amelioration of the phenocopies of *PLCβ* and *Gαs* morphants by GABA (Figure 5G and H).

The constitutive function of wild-type Gαq

We found that *Ciona* wild-type Gαq (wtGαq) has constitutive activity. In contrast to wt*Gαs* and wt*Gαi*, overexpression of wt*Gαq* did not arrest metamorphosis (Figure S6A). Rather, its overexpression induced metamorphosis without settlement (Figure S6B). The constitutive wt*Gαq* activity was confirmed by the rescue of *Gαs* morphants (Figure S6C). As mentioned above, caGαq also has these activities (Figure 1L). ca*Gαq*-overexpressed larvae had a somewhat rounder trunk shape, abnormal tail bending, and frequent tail twitching, perhaps due to a constitutive increase in the cytosolic Ca^{2+} concentration (Figure S6D). Overexpression of wt*Gαq* did not show such abnormalities

(Figure S6E), suggesting that wtGαq has milder activity than, or works through a different mechanism from, caGαq. To gain further insight into the constitutive effect of wtGαq, we constructed a dominant-negative form of Gαq[66] that has reduced GDP/GTP binding activity while maintaining βγ binding activity. Overexpression of dn*Gαq* weakly inhibited metamorphosis (Figure S6F), suggesting that GDP/GTP exchange is important for the constitutive activity of wtGαq.

Discussion

Among chordates, the tunicate ascidian is the only group that exhibits a sessile lifestyle at the adult stage. Understanding how ascidians acquired the mechanism to metamorphose into sessile adults is important for elucidating the evolution of chordates[75,76]. Through extensive molecular, physiological, and pharmacological analyses, we identified signaling molecules responsible for the initiation of metamorphosis of the ascidian *Ciona*. Combining the results with previous knowledge, we described a schematic that best represents the cascades running in the adhesive papillae upon adhesion to initiate metamorphosis (Figure 7). This working hypothesis will be the basis for future research on ascidian/tunicate metamorphosis. The hypothesis explains the characteristics of *Ciona* metamorphosis, the mechanisms of which have not yet been elucidated. The genes, proteins, and signaling pathways in this schematic are essential targets for elucidating how the ancestor of ascidians acquired the metamorphosis system peculiar to this group during evolution.

Mechanisms measuring duration and strength of adhesions

One mystery of *Ciona* metamorphosis is that its initiation requires continuous adhesion with the adhesive organ for a certain period. This requirement is suggested for the faithful achievement of metamorphosis only when adhesion is firm enough to allow the transition out of the free-living larval stage. Our previous study suggested that approximately 30 min of adhesion is necessary[27]. A shorter duration of adhesion does not trigger metamorphosis. Larvae that experience short-term adhesion (such as detaching before 30 min) need to adhere again for 30 min to initiate metamorphosis, suggesting that the experience of temporal adhesion is erased. Our recent study showed that the force given to the papillae by adhesion also affects metamorphosis initiation: weaker force extends the time requirement[22]. Therefore, *Ciona* larvae likely possess a mechanism that somehow measures the duration and strength of adhesion and the ability to cancel transient excitations of the adhesive organ. Because fewer than 300 neurons constitute the larval nervous system of *Ciona*[54,55,77], how the larva measures the strength and duration of adhesion with its simple nervous system is an important question to address the mechanisms of metamorphosis.

This study showed that cAMP is an essential second messenger molecule for triggering metamorphosis. Because PDE constitutively degrades cAMP, accumulation of this molecule requires persistent and/or strong activation of the metamorphic pathway that overcomes PDE activity. In other words, the duration and strength of adhesion could be converted into the quantity of cAMP, and when its quantity reaches a threshold, metamorphosis can be initiated. The time between the start of adhesion and metamorphosis initiation may be the period necessary to accumulate sufficient cAMP. This “cAMP timer” mechanism does not demand a complicated neuronal network system and could work in the simple nervous system of *Ciona*.

G-protein signaling relay for metamorphosis

This study showed that three major G-proteins are involved in the initiation of metamorphosis (Figure 7). This complicated mechanism contrasts the simple determination of metamorphosis initiation by cAMP accumulation. What factor promoted the ancestor of ascidians to acquire this complicated signaling network of metamorphosis? We suspect that incorporating multiple components increases the chance of generating the crosstalk between molecules, providing rigidity and flexibility to the system. Particularly, the involvement of Gi may have been important for achieving metamorphosis at the correct time and condition. GABA and Gi have inhibitory and excitatory functions[78,79]. As we discussed, *Ciona* larvae must ignore transient adhesion or stimulation on the papilla, which may occur frequently during swimming by colliding with an object or by strong water flows. At the same time, larvae must maintain sensing ability and start metamorphosis when they encounter an appropriate stimulus. Through the GIRK channel and Gαi, GABA can suppress the excitation and cAMP accumulation in the papilla. The GIRK channel could increase the excitation threshold of papilla neurons, allowing them to ignore weak stimuli. The transient reduction of cAMP (Figure 3E) after papilla stimulation guarantees the requirement of long-time adhesion irrespective of the initial quantity of cAMP. This cAMP reduction could be partly explained by the inhibitory function of Gαi on ACs. PDE1 is known to be activated by Ca^{2+}/calmodulin[80]. Because PDE1 is abundantly expressed in the papillae, the increase in Ca^{2+} upon adhesion could also trigger sudden cAMP reduction through PDE1.

Together with its inhibitory function, GABA can activate the Gq pathway,

which promotes metamorphosis through Gβγi. Group III AC and MEK could also be the targets of Gβγi. When adhesion is long enough, their activations somehow overcome the inhibitory functions of GABA. The GABA pathway is an ideal player that fulfills multiple requirements in the regulation of metamorphosis through its excitatory and inhibitory functions. We suspect that papillae themselves are the source of GABA for metamorphosis initiation. Because VIAAT/VGAT is not expressed in the papillae, the secretion of GABA from the papilla neurons requires an atypical mechanism. GABA is detected in the cell body of the neurons[19]. The release of cytosolic GABA may be triggered by the reception of mechanical stimuli using the TRP channel[22]. A VIAAT-independent cytosolic GABA release is observed in pancreatic beta cells[81]. Curiously, papilla neurons express transcription factor Islet[82].

GPCRs for initiating metamorphosis and atypical Gαq activity

Future studies need to specify the mechanisms underlying Gαi, Gαq, and Gαs activation as well as the interaction between them more precisely. The activation of trimeric G-proteins relies on GPCRs, suggesting the presence of the receptors coupled with Gi, Gq, and Gs for metamorphosis initiation (Figure 7). Among them, Gi is likely to be coupled with GABABR; however, the expression of GABABR in the papillae is weak, and their interaction needs to be clarified in the future. We found that wild-type Gαq exhibits constitutive activity that does not require activation through adhesion. The constitutive Gαq activity requires GTP binding. If a GPCR owns this Gαq activation, its ligand should be supplied constitutively. Wild-type *Ciona* does not initiate metamorphosis without adhesion even though Gαq is expressed in the adhesive papillae, suggesting that the quantity of Gαq is strictly regulated to prevent autonomous

metamorphosis in normal conditions.

We did not identify the GPCR coupled with Gs in the metamorphic mechanism. We suspect that GnRH receptors (GnRHRs) are strong candidates for this role. Our previous studies showed that GnRHs can induce metamorphosis[36,37] as a downstream factor of GABA. Among the four genes encoding GnRHR proteins, *GnRHR1* and *GnRHR2* are expressed in the adhesive papillae[83]. These GnRHRs stimulate cAMP signaling, and the ligand GnRHs for GnRHR1 are also expressed in the papillae[83–85]. Therefore, GnRHs could be secreted from adhesive papillae as downstream molecules of GABA and stimulate the Gs pathway through GnRHR1. Future studies targeting the regulation of the secretion and reception of GnRH peptides after stimulation of papillae will improve our understanding of the signaling cascade conducting *Ciona* metamorphosis.

Understanding whether the G-protein signaling relay occurs in cell-autonomous or non-autonomous fashions is crucial for deepening our understanding of *Ciona* metamorphosis. Each papilla comprises approximately 20 cells, including four papilla neurons (PNs). We showed that activation of Gq and Gs pathways in PNs is sufficient for initiating metamorphosis. This coincides with the previous reports[22,23] that the loss of PNs by disrupting the POUIV transcription factor caused the complete arrest of metamorphosis. However, we do not think PNs are the only cells that activate G-proteins, because Ca^{2+} and cAMP imaging showed upregulation of fluorescence in the entire papillae[16,22]. A recent study also reports Ca^{2+} transient in another cell type than PNs[34]. Other papilla cells are likely responsible for activating G-proteins by directly responding to adhesion and by receiving signal input from adjacent cells, thereby enhancing the signal strength to accumulate a sufficient quantity of cAMP in the PNs to

initiate metamorphosis. In this study, technical limitations prevented us from characterizing cells exhibiting increases in Ca^{2+} and cAMP; we need to address this question in future studies.

Evolutionary implications

Sessile or benthic marine invertebrates lose locomotive activity when they undergo metamorphosis triggered by adhesion to a substratum[86]. These animals are suspected of having a system to control the adhesion state, allowing them to repeat attachment and detachment before meeting the appropriate conditions for metamorphosis. For example, barnacle larvae "walk" on the substratum before adhering firmly by secreting cement[87]. Like *Ciona*, the larvae of sessile/benthic animals may have a system to initiate metamorphosis only when appropriate adhesion is provided, while erasing stimuli from transient and inappropriate adhesion. GABA serves as the metamorphosis inducer of some benthic invertebrates, including mollusks and echinoderms[88–90]. Moreover, GPCR is implicated as the mediator of settlement and metamorphosis induction in hydrozoans, mollusks, and barnacles[88,91,92]. In the abalone and barnacle, the dual use of Gq and Gs pathways in metamorphosis has been suggested[93,94]. Supported by these shared features in the metamorphic mechanisms, our working hypothesis about the initiation of *Ciona* metamorphosis (Figure 7) will serve as a cue to elucidate how marine benthic invertebrates regulate their metamorphosis.

Materials and Methods

Animals

Ciona intestinalis Type A wild types collected from Onagawa Bay (Miyagi, Japan) and Onahama Bay (Fukushima, Japan) were cultivated in closed colonies by the staff of the National BioResource Project, Japan. They were kept under a constant light condition to prevent gamete release. Eggs and sperm were collected surgically from gonadal ducts, and insemination was carried out in dishes. To prevent larvae from initiating metamorphosis, the tail's posterior half was manually cut with a scalpel. Removing the tail prevents larvae from swimming efficiently, and these larvae are usually unable to adhere to a substrate. These adhesion-prevented larvae do not metamorphose, since adhesion is required to initiate metamorphosis. Larvae developed from dechorionated eggs were cultured on a 2% agar-coated dish after tail amputation to prevent metamorphosis. Because larvae stick to plastics, tail amputation is insufficient to avoid their adhesion to the culture dish.

Pharmacological treatment

Larvae or larval anterior fragments isolated with a scalpel were administered overnight with 700 μM GABA (Fujifilm Wako #010-02441) or 1 mM theophylline (Sigma-Aldrich #T1633) dissolved in seawater, or 4 μM U0126 (Promega #V1121) dissolved in DMSO.

Plasmids

The open reading frame (ORF) of Kaede was removed from pSPCiPC2Kaede by inverse PCR with PrimeStar GxL DNA polymerase (Takara-bio #R050). The ORFs of *Gαq*, *Gαs*, *Gαi*, and *PLCβ1/2/3* were PCR amplified using full-insert cDNAs[95]. These PCR fragments were fused with the In-Fusion HD Cloning kit (Clontech #639650). The

region encoding XY linker[43] was deleted from *PLCβ1/2/3* cDNA by inverse PCR to create a constitutively active form. The mutations were introduced by inverse PCR to create constitutive active or dominant-negative forms of *Gα* cDNAs. The introduced mutations are as follows: ca*Gαq*, corresponding to Q223L, abolishes GTPase activity[42]; ca*Gαs*, corresponding to Q227L, abolishes GTPase activity[47]; dn*Gαi*, corresponding to S47C[66,67]; and dn*Gαq*, corresponding to S54N[66]. The ORF of *bPAC*[51] was PCR amplified and inserted between the *Bam*HI and *Eco*RI restriction sites of pSP-Kaede[96] to create pSPbPAC. The PCR-amplified *PC2 cis*-element[46] was inserted into the *Bam*HI site of pSPbPAC. The plasmid DNAs were linearized by a restriction enzyme and purified with the Qiaquick Gel Extraction Kit (Qiagen #28706) before microinjection. The ORF of *Pink Flamindo*[52] was PCR amplified and inserted into the *Eco*RV restriction sites of pBS-HTB[97,98] to create pHTBPinkFlamindo. The plasmids pHTBGCaMP8[22] and pHTBPinkFlamindo were linearized using *Xho*I for subsequent *in vitro* synthesis of *GCaMP8* and *Pink Flamindo* mRNA, respectively. *GCaMP8* mRNA was synthesized with the MEGAscript T3 kit (Thermo Fisher Scientific #AM1338), the Poly (A) Tailing kit (Thermo Fisher Scientific #AM1350), and the Cap structure analog (New England Biolabs #S1404). Pink Flamindo mRNA was synthesized with the mMESSAGE mMACHINE T3 Transcription kit (Thermo Fisher Scientific #AM1348).

Microinjection

Unfertilized eggs were dechorionated in sterilized seawater containing 1% sodium thioglycolate (Fujifilm Wako #590-11762) and 0.05% actinase E (Kaken Pharmaceutical #650164) as previously described[99]. The microinjection solution included 2 mg/ml of Fast Green FCF (Fujifilm Wako #061-00031), 0.5-1.0 mM of

morpholino oligonucleotide(s) (MOs)[100], 5 ng/ul of plasmids, and/or 1 mg/ml of *GCaMP8* mRNA for imaging[22]. For cAMP imaging, 1 mg/ml *Pink Flamindo* mRNA was dissolved in water without Fast Green, since this chemical emits fluorescence. Microinjected unfertilized eggs were inseminated in a gelatin-coated plastic dish. After the seawater was exchanged to remove excess sperm, the fertilized eggs were cultured at 18 ºC or 20 ºC overnight until the larval stage. MOs are listed below. Standard control MO, 5'- CCTCTTACCTCAGTTACAATTTATA-3'; *GAD* ATG MO[36], 5'-ACCTCCAAGCCGATTGTTTCTGCAT-3'; *GABABR1* ATG MO[36], 5'-GCTTACGACTTTACATAACCTTACA-3'; *Gαq* ATG MO, 5'-GGCATATTTGTGACTATAATGACG-3'; *Gαs* ATG MO, 5'-AAAGCAACCCATTGGCATTATCGAC-3'; *PLCβ1/2/3* splicing MO, 5'-GTGTTACTTACGCTTTCTCTA-3'; *PLCβ4* splicing MO, 5'-AACCACCAACCACCAACCTTTTG-3'; *IP3R* splicing MO, 5'-AATGATGGTTTAAAATTGCCACCTG-3'; *Gαi* ATG MO, 5'-GTGGAGACTGTGCAACCCATGATTC-3'; *dvGai_Chr2* ATG MO, 5'-CCATCTTGAGTAATCCAGGCTTTTA-3'; *GIRK channel* ATG MO, 5'-TCTGCTGGTTCAGTAATAGACATAG-3'.

Photographing and imaging

Photographs were taken with an AxioImager Z1 and AxioObserver Z1 (Carl Zeiss). The images were treated with AxioVision Rel.4.6 or Zen (Carl Zeiss) and Photoshop 2021 (Adobe) software. Imaging of the Ca^{2+} transient was carried out according to previous reports[16,22]. The tails of *GCaMP8* mRNA-injected larvae were removed by a scalpel at 15-17 hours after fertilization (hpf). At 30-40 hpf, the larvae were mounted onto a

plastic dish under an M165FC stereo microscope (Leica Microsystems), and their adhesive papillae were stimulated by a glass rod using a three-axis coarse manipulator M-152 (Narishige Japan). Immediately after the tip of the rod had contact with the papillae, visible light was shut off and the fluorescence of GCaMP8 was taken with a DFC 310FX digital camera (Leica), Las version 4.12 (Leica), and the movie-capturing function of Windows 10. Images were treated with Photoshop 2021.

Imaging of cAMP was taken by confocal laser scanning microscopy (FV1000, Olympus). The movies were treated with ImageJ (National Institutes of Health). The Pink Flamindo mRNA-injected larvae were immobilized on Poly L lysine-coated glass-bottom dishes at 20-21 hpf. For stimulation of their adhesive papillae with a glass rod, an electric manipulator MM-89 (Narishige) and hydraulic micromanipulator MMO-202ND (Narishige) were used.

RNA sequencing

Larval anterior portions, including adhesive papillae and the other trunk region, were separately isolated by a scalpel around 22-25 hpf at 18°C and collected in Isogen (Nippon Gene #317-02503) soon after isolation. To identify GABA-responsive genes, half of the tail was amputated from larvae around 21-24 hpf, followed by GABA administration for 2 hours before treatment with Isogen. In each experiment, approximately 50 fragments were collected, and two biological replicates were taken. Total RNA was isolated according to the manufacturer's instructions. Ribosomal RNA was depleted from the total RNA using the NEBNext rRNA Depletion kit (New England Biolabs #E6310), followed by the conversion of the remaining RNA into an Illumina sequencing library using the NEBNext Ultra Directional RNA Library Prep kit

(New England Biolabs #E7760). Following library preparation, validation was performed using the Bioanalyzer system (Agilent Technologies) to assess size distribution and concentration. Subsequently, sequencing was carried out on the NextSeq 500 platform (Illumina) employing the paired-end 36-base read option. Reads were mapped on the *Ciona intestinalis* Type A reference genome (HT model; http://ghost.zool.kyoto-u.ac.jp/default_ht.html) and quantified using CLC Genomic Workbench version 22.0 (Qiagen). RNA-seq data sets were deposited in the NCBI Gene Expression Omnibus (GEO) under accession numbers SAMN40712866 to SAMN40712873, which will appear online upon publication of this paper.

The read counts were normalized by calculating the number of reads per kilobase per million (RPKM) for each transcript in each sample using CLC Genomic Workbench version 22.0 (Qiagen). Eight candidate genes showing a minimum 1.5-fold increase following GABA administration, along with notably higher expression in the papillae in comparison to the trunk (an approximately 4-fold increase in a sample), were chosen for quantitative PCR analysis to assess their response to GABA.

Quantitative PCR

Total RNA was isolated from the anterior tips of larvae treated with the chemical using Isogen (Nippon Gene), following the manufacturer's instructions. After isopropanol extraction, genomic DNA removal and reverse transcription were carried out using the PrimeScript™ RT reagent kit with gDNA Eraser (Takara Bio #RR047). Quantitative RT-PCR (qRT-PCR) was done using a SYBR Premix Ex TaqII Dimer Eraser (Takara Bio #RR091) and a Thermal Cycler Dice Real Time System III (Takara Bio). The gene encoding elongation factor 1α (*EF1α*) was used to normalize RNA quantity according

to a previous study[98]. qPCR primers are listed below. KY21.Chr5.240, 5'-TCTTCTCAAAGTTGCACATTCC-3' and 5'-CAGCAGCAACCAAACGATAAAC-3'; KY21.Chr8.489, 5'- CAATGCAACTTTGACTGCATAC-3' and 5'-TCCAAACTGCATTCCACATATC-3'; *EF1α*, 5'-CATGTCACGGACAGCGAAACG-3' and 5'- CAATGTGTGTTGAGGCATTCCAAG-3'.

Statistical analysis

Differences between conditions were evaluated by Fisher's exact test. Statistical analyses and most graph visualizations were conducted utilizing R x64.4.1.2 and RStudio software.

Phylogenetic analysis

We performed a tBlastn search[101] against the HT gene model of *Ciona*[61] using the amino acid sequences of human PDE, PLCβ, and *Ciona* Gα proteins as queries, followed by a reciprocal Blast search. We aligned the amino acid sequences from the HDc domain of PDE, the EF-hand_like, PLCXc, PLCYc, and C2 domains of PLCβ, and the whole open reading frame of Gα proteins using the M-COFFEE program[102,103]. After the removal of unnecessary residues, maximum likelihood trees were constructed using MEGA software version 11[104], employing the WAG amino acid substitution matrix[105]. The trees were assessed with 1,000 bootstrap pseudoreplicates.

Acknowledgements

We would like to express our earnest gratitude to Drs. Kazuki Horikawa, Atsuo Nishino,

Ryusuke Niwa, and Takahiro Yamashita for their kind material provision, helpful comments, and general support of our study. We thank Dr. Kogiku Shiba for instructing us with the pharmacological analyses. We also thank Dr. Masafumi Muratani and members of i-Laboratory at the University of Tsukuba for their support for RNA sequencing. We are grateful to the past and present members of the Shimoda Marine Research Center at the University of Tsukuba for their contributions to the initial step of this study and the maintenance of the animals. We thank Drs. Shigeki Fujiwara, Manabu Yoshida, Yutaka Satou, and all members of the Department of Zoology, Kyoto University, the Misaki Marine Biological Station, the University of Tokyo, the Maizuru Fishery Research Station of Kyoto University, and the National BioResource Project (NBRP) for the cultivation and provision of *Ciona* adults and experimental materials. This study was supported by grants from the Japan Society for the Promotion of Science to K.H. (21H00440, 23H04717), T.H. (19H03204, 21K19249, 21H05239), and Y.S. (19H03262). Y.S. was further supported by a Takeda Bioscience Research Grant. T.H. was supported by the Collaborative Research in Computational Neuroscience program (CRCNS2021). N.M.T was supported by JST SPRING (JPMJSP2123).

Author Contributions

A.H., N.M.T., A.O., Y.W., and Y.S. performed the experiments. Y.S. designed the experiments. T.H., M.H., and A.S. performed RNA-seq data and phylogenetic analyses. H.S., T.H., and K.H. supervised the work. Y.S. wrote the manuscript with consultations by A.H., N.M.T., and K.H. All authors contributed to the manuscript preparation.

References

1. Barresi, M.J.F., and Gilbert, S.F. (2020). Developmental Biology (Oxford University Press).

2. Arenas-Mena, C. (2010). Indirect development, transdifferentiation and the macroregulatory evolution of metazoans. Philos. Trans. R. Soc. Lond. B Biol. Sci. *365*, 653–669.

3. Hadfield, M.G., Carpizo-Ituarte, E.J., del Carmen, K., and Edved, B.T.N. (2001). Metamorphic Competence, a Major Adaptive Convergence in Marine Invertebrate Larvae1. A MER .Z OOL *41*, 1123–1131.

4. Degnan, S.M., and Degnan, B.M. (2010). The initiation of metamorphosis as an ancient polyphenic trait and its role in metazoan life-cycle evolution. Philos. Trans. R. Soc. Lond. B Biol. Sci. *365*, 641–651.

5. Williams, E.A., Cummins, S., and Degnan, S.M. (2009). Effective induction of abalone settlement and metamorphosis corresponds to biomolecular composition of natural cues. Commun. Integr. Biol. *2*, 347–349.

6. Say, T.E., and Degnan, S.M. (2020). Molecular and behavioural evidence that interdependent photo - and chemosensory systems regulate larval settlement in a marine sponge. Mol. Ecol. *29*, 247–261.

7. Yap, F.-C., Chen, H.-N., and Chan, B.K.K. (2023). Host specificity and adaptive evolution in settlement behaviour of coral-associated barnacle larvae (Cirripedia: Pyrgomatidae). Sci. Rep. *13*, 9668.

8. Delsuc, F., Brinkmann, H., Chourrout, D., and Philippe, H. (2006). Tunicates and not cephalochordates are the closest living relatives of vertebrates. Nature *439*, 965–968.

9. Satoh, N. (2003). The ascidian tadpole larva: comparative molecular development and genomics. Nat. Rev. Genet. *4*, 285–295.

10. Nishino, A., Baba, S.A., and Okamura, Y. (2011). A mechanism for graded motor control encoded in the channel properties of the muscle ACh receptor. Proc. Natl.

Acad. Sci. U. S. A. *108*, 2599–2604.

11. Horie, T., Nakagawa, M., Sasakura, Y., Kusakabe, T.G., and Tsuda, M. (2010). Simple motor system of the ascidian larva: neuronal complex comprising putative cholinergic and GABAergic/glycinergic neurons. Zoolog. Sci. *27*, 181–190.

12. Karaiskou, A., Swalla, B.J., Sasakura, Y., and Chambon, J.-P. (2015). Metamorphosis in solitary ascidians. Genesis *53*, 34–47.

13. Hotta, K., Dauga, D., and Manni, L. (2020). The ontology of the anatomy and development of the solitary ascidian Ciona: the swimming larva and its metamorphosis. Sci. Rep. *10*, 17916.

14. Cloney, R.A. (1982). Ascidian larvae and the events of metamorphosis. Am. Zool. *22*, 817–826.

15. Zeng, F., Wunderer, J., Salvenmoser, W., Hess, M.W., Ladurner, P., and Rothbächer, U. (2019). Papillae revisited and the nature of the adhesive secreting collocytes. Dev. Biol. *448*, 183–198.

16. Wakai, M.K., Nakamura, M.J., Sawai, S., Hotta, K., and Oka, K. (2021). Two-Round Ca2+ transient in papillae by mechanical stimulation induces metamorphosis in the ascidian Ciona intestinalis type A. Proceedings of the Royal Society B *288*. 10.1098/rspb.2020.3207.

17. Takamura-Neural cells.pdf. Preprint.

18. Horie, T., Kusakabe, T., and Tsuda, M. (2008). Glutamatergic networks in the Ciona intestinalis larva. J. Comp. Neurol. *508*, 249–263.

19. Brown, E.R., Nishino, A., Bone, Q., Meinertzhagen, I.A., and Okamura, Y. (2005). GABAergic synaptic transmission modulates swimming in the ascidian larva. Eur. J. Neurosci. *22*, 2541–2548.

20. Chacha, P.P., Horie, R., Kusakabe, T.G., Sasakura, Y., Singh, M., Horie, T., and Levine, M. (2022). Neuronal identities derived by misexpression of the POU IV sensory determinant in a protovertebrate. Proc. Natl. Acad. Sci. U. S. A. *119*. 10.1073/pnas.2118817119.

21. Nakayama-Ishimura, A., Chambon, J.-P., Horie, T., Satoh, N., and Sasakura, Y.

(2009). Delineating metamorphic pathways in the ascidian Ciona intestinalis. Dev. Biol. *326*, 357–367.

22. Sakamoto, A., Hozumi, A., Shiraishi, A., Satake, H., Horie, T., and Sasakura, Y. (2022). The TRP channel PKD2 is involved in sensing the mechanical stimulus of adhesion for initiating metamorphosis in the chordate Ciona. Dev. Growth Differ. *64*, 395–408.

23. Johnson, C.J., Kulkarni, A., Buxton, W.J., Hui, T.Y., Kayastha, A., Khoja, A.A., Leandre, J., Mehta, V.V., Ostrowski, L., Pareizs, E.G., et al. (2023). Using CRISPR/Cas9 to identify genes required for mechanosensory neuron development and function. Biol. Open *12*. 10.1242/bio.060002.

24. Caputi, L., Andreakis, N., Mastrototaro, F., Cirino, P., Vassillo, M., and Sordino, P. (2007). Cryptic speciation in a model invertebrate chordate. Proc. Natl. Acad. Sci. U. S. A. *104*, 9364–9369.

25. Pennati, R., Ficetola, G.F., Brunetti, R., Caicci, F., Gasparini, F., Griggio, F., Sato, A., Stach, T., Kaul-Strehlow, S., Gissi, C., et al. (2015). Morphological Differences between Larvae of the Ciona intestinalis Species Complex: Hints for a Valid Taxonomic Definition of Distinct Species. PLoS One *10*, e0122879.

26. Brunetti, R., Gissi, C., Pennati, R., Caicci, F., Gasparini, F., and Manni, L. (2015). Morphological evidence that the molecularly determined*Ciona intestinalis*type A and type B are different species:*Ciona robusta*and*Ciona intestinalis*. J. Zoolog. Syst. Evol. Res. *53*, 186–193.

27. Matsunobu, S., and Sasakura, Y. (2015). Time course for tail regression during metamorphosis of the ascidian Ciona intestinalis. Dev. Biol. *405*, 71–81.

28. Patricolo, E., Cammarata, M., and D'Agati, P. (2001). Presence of thyroid hormones in ascidian larvae and their involvement in metamorphosis. J. Exp. Zool. *290*, 426–430.

29. Arnold, J., Eri, R., Degnan, B., and Lavin, M. (1997). Novel gene containing multiple epidermal growth factor–like motifs transiently expressed in the papillae of the ascidian tadpole larvae. Dev. Dyn. *210*. 10.1002/(SICI)1097-0177(199711)210:3<264::AID-AJA7>3.0.CO;2-E.

30. Coniglio, L., Morale, A., Angelini, C., and Falugi, C. (1998). Cholinergic activation of settlement in Ciona intestinalis metamorphosing larvae. J. Exp. Zool. *280*, 314–320.

31. Eri, R., Arnold, J.M., Hinman, V.F., Green, K.M., Jones, M.K., Degnan, B.M., and Lavin, M.F. (1999). Hemps, a novel EGF-like protein, plays a central role in ascidian metamorphosis. Development *126*, 5809–5818.

32. Kimura, Y., Yoshida, M., and Morisawa, M. (2003). Interaction between noradrenaline or adrenaline and the beta 1-adrenergic receptor in the nervous system triggers early metamorphosis of larvae in the ascidian, Ciona savignyi. Dev. Biol. *258*, 129–140.

33. Zega, G., Pennati, R., Groppelli, S., Sotgia, C., and De Bernardi, F. (2005). Dopamine and serotonin modulate the onset of metamorphosis in the ascidian Phallusia mammillata. Dev. Biol. *282*, 246–256.

34. Hoyer, J., Kolar, K., Athira, A., van den Burgh, M., Dondorp, D., Liang, Z., and Chatzigeorgiou, M. (2024). Polymodal sensory perception drives settlement and metamorphosis of Ciona larvae. Curr. Biol. *34*, 1168-1182.e7.

35. Patricolo, E., Ortolani, G., and Cascio, A. (1981). The effect of l-thyroxine on the metamorphosis of Ascidia malaca. Cell Tissue Res. *214*, 289–301.

36. Hozumi, A., Matsunobu, S., Mita, K., Treen, N., Sugihara, T., Horie, T., Sakuma, T., Yamamoto, T., Shiraishi, A., Hamada, M., et al. (2020). GABA-Induced GnRH Release Triggers Chordate Metamorphosis. Curr. Biol. *30*, 1555-1561.e4.

37. Kamiya, C., Ohta, N., Ogura, Y., Yoshida, K., Horie, T., Kusakabe, T.G., Satake, H., and Sasakura, Y. (2014). Nonreproductive role of gonadotropin-releasing hormone in the control of ascidian metamorphosis. Dev. Dyn. *243*, 1524–1535.

38. Shaye, H., Stauch, B., Gati, C., and Cherezov, V. (2021). Molecular mechanisms of metabotropic GABAB receptor function. Sci. Adv. *7*, eabg3362.

39. Alberts, B. (2017). Molecular biology of the cell 6th ed. (Garland Science).

40. Prasobh, R., and Manoj, N. (2009). The repertoire of heterotrimeric G proteins and RGS proteins in Ciona intestinalis. PLoS One *4*, e7349.

41. Harden, T.K., Waldo, G.L., Hicks, S.N., and Sondek, J. (2011). Mechanism of activation and inactivation of Gq/phospholipase C-β signaling nodes. Chem. Rev. *111*, 6120–6129.

42. Oki, K., Fujisawa, Y., Kato, H., and Iwasaki, Y. (2005). Study of the constitutively active form of the alpha subunit of rice heterotrimeric G proteins. Plant Cell Physiol. *46*, 381–386.

43. Charpentier, T.H., Waldo, G.L., Barrett, M.O., Huang, W., Zhang, Q., Harden, T.K., and Sondek, J. (2014). Membrane-induced Allosteric Control of Phospholipase C-β Isozymes*. J. Biol. Chem. *289*, 29545–29557.

44. Yokoyama, T.D., Hotta, K., and Oka, K. (2014). Comprehensive morphological analysis of individual peripheral neuron dendritic arbors in ascidian larvae using the photoconvertible protein Kaede. Dev. Dyn. *243*, 1362–1373.

45. Osugi, T., Sasakura, Y., and Satake, H. (2020). The ventral peptidergic system of the adult ascidian Ciona robusta (Ciona intestinalis Type A) insights from a transgenic animal model. Sci. Rep. *10*, 1892.

46. Osugi, T., Sasakura, Y., and Satake, H. (2017). The nervous system of the adult ascidian Ciona intestinalis Type A (Ciona robusta): Insights from transgenic animal models. PLoS One *12*, e0180227.

47. Kelly, M.P., Isiegas, C., Cheung, Y.-F., Tokarczyk, J., Yang, X., Esposito, M.F., Rapoport, D.A., Fabian, S.A., Siegel, S.J., Wand, G., et al. (2007). Constitutive activation of Galphas within forebrain neurons causes deficits in sensorimotor gating because of PKA-dependent decreases in cAMP. Neuropsychopharmacology *32*, 577–588.

48. Neves, S.R., Ram, P.T., and Iyengar, R. (2002). G protein pathways. Science *296*, 1636–1639.

49. Essayan, D.M. (2001). Cyclic nucleotide phosphodiesterases. J. Allergy Clin. Immunol. *108*, 671–680.

50. Daly, J.W., Ukena, D., and Jacobson, K.A. (1987). Analogues of Adenosine, Theophylline, and Caffeine: Selective Interactions with A1 and A2 Adenosine Receptors. In Topics and Perspectives in Adenosine Research (Springer Berlin

Heidelberg), pp. 23–36.

51. Stierl, M., Stumpf, P., Udwari, D., Gueta, R., Hagedorn, R., Losi, A., Gärtner, W., Petereit, L., Efetova, M., Schwarzel, M., et al. (2011). Light modulation of cellular cAMP by a small bacterial photoactivated adenylyl cyclase, bPAC, of the soil bacterium Beggiatoa. J. Biol. Chem. *286*, 1181–1188.

52. Harada, K., Ito, M., Wang, X., Tanaka, M., Wongso, D., Konno, A., Hirai, H., Hirase, H., Tsuboi, T., and Kitaguchi, T. (2017). Red fluorescent protein-based cAMP indicator applicable to optogenetics and in vivo imaging. Sci. Rep. *7*, 7351.

53. Zega, G., Biggiogero, M., Groppelli, S., Candiani, S., Oliveri, D., Parodi, M., Pestarino, M., De Bernardi, F., and Pennati, R. (2008). Developmental expression of glutamic acid decarboxylase and of gamma-aminobutyric acid type B receptors in the ascidian Ciona intestinalis. J. Comp. Neurol. *506*, 489–505.

54. Ryan, K., Lu, Z., and Meinertzhagen, I.A. (2016). The CNS connectome of a tadpole larva of Ciona intestinalis (L.) highlights sidedness in the brain of a chordate sibling. Elife *5*. 10.7554/eLife.16962.

55. Ryan, K., Lu, Z., and Meinertzhagen, I. (2018). The peripheral nervous system of the ascidian tadpole larva: Types of neurons and their synaptic networks. J. Comp. Neurol. *526*, 583–608.

56. Sadana, R., and Dessauer, C.W. (2009). Physiological roles for G protein-regulated adenylyl cyclase isoforms: insights from knockout and overexpression studies. Neurosignals *17*, 5–22.

57. Cooper, D.M.F. (2015). Store-operated Ca^{2+}-entry and adenylyl cyclase. Cell Calcium *58*, 368–375.

58. Karls, A., and Mynlieff, M. (2015). GABA(B) receptors couple to Gαq to mediate increases in voltage-dependent calcium current during development. J. Neurochem. *135*, 88–100.

59. Shen, C., Mao, C., Xu, C., Jin, N., Zhang, H., Shen, D.-D., Shen, Q., Wang, X., Hou, T., Chen, Z., et al. (2021). Structural basis of GABAB receptor-Gi protein coupling. Nature *594*, 594–598.

60. Yoshida, R., Sakurai, D., Horie, T., Kawakami, I., Tsuda, M., and Kusakabe, T. (2004). Identification of neuron-specific promoters in Ciona intestinalis. Genesis *39*, 130–140.

61. Satou, Y., Tokuoka, M., Oda-Ishii, I., Tokuhiro, S., Ishida, T., Liu, B., and Iwamura, Y. (2022). A Manually Curated Gene Model Set for an Ascidian, Ciona robusta (Ciona intestinalis Type A). Zoolog. Sci. *39*. 10.2108/zs210102.

62. Conklin, B.R., Farfel, Z., Lustig, K.D., Julius, D., and Bourne, H.R. (1993). Substitution of three amino acids switches receptor specificity of Gqα to that of Giα. Nature *363*, 274–276.

63. Tu, H., Xu, C., Zhang, W., Liu, Q., Rondard, P., Pin, J.-P., and Liu, J. (2010). $GABA_B$receptor activation protects neurons from apoptosis via IGF-1 receptor transactivation. J. Neurosci. *30*, 749–759.

64. Mizuta, K., Mizuta, F., Xu, D., Masaki, E., Panettieri, R.A., Jr, and Emala, C.W. (2011). Gi-coupled γ-aminobutyric acid-B receptors cross-regulate phospholipase C and calcium in airway smooth muscle. Am. J. Respir. Cell Mol. Biol. *45*, 1232–1238.

65. Sankaran, B., Osterhout, J., Wu, D., and Smrcka, A.V. (1998). Identification of a Structural Element in Phospholipase C β2 That Interacts with G Protein βγ Subunits*. J. Biol. Chem. *273*, 7148–7154.

66. Barren, B., and Artemyev, N.O. (2007). Mechanisms of dominant negative G - protein α subunits. J. Neurosci. Res. *85*, 3505–3514.

67. Slepak, V.Z., Katz, A., and Simon, M.I. (1995). Functional analysis of a dominant negative mutant of Gαi2. J. Biol. Chem. *270*, 4037–4041.

68. Dascal, N., and Kahanovitch, U. (2015). The roles of Gβγ and Gα in gating and regulation of GIRK channels. In International Review of Neurobiology International review of neurobiology. (Elsevier), pp. 27–85.

69. Blaukat, A., Barac, A., Cross, M.J., Offermanns, S., and Dikic, I. (2000). G protein-coupled receptor-mediated mitogen-activated protein kinase activation

through cooperation of Galpha(q) and Galpha(i) signals. Mol. Cell. Biol. *20*, 6837–6848.

70. Chambon, J.-P., Soule, J., Pomies, P., Fort, P., Sahuquet, A., Alexandre, D., Mangeat, P.-H., and Baghdiguian, S. (2002). Tail regression in Ciona intestinalis (Prochordate) involves a Caspase-dependent apoptosis event associated with ERK activation. Development *129*, 3105–3114.

71. Chambon, J.-P., Nakayama, A., Takamura, K., McDougall, A., and Satoh, N. (2007). ERK- and JNK-signalling regulate gene networks that stimulate metamorphosis and apoptosis in tail tissues of ascidian tadpoles. Development *134*, 1203–1219.

72. Kim, G.J., and Nishida, H. (2001). Role of the FGF and MEK signaling pathway in the ascidian embryo. Dev. Growth Differ. *43*, 521–533.

73. Hudson, C., Darras, S., Caillol, D., Yasuo, H., and Lemaire, P. (2003). A conserved role for the MEK signalling pathway in neural tissue specification and posteriorisation in the invertebrate chordate, the ascidian Ciona intestinalis. Development *130*, 147–159.

74. Goldsmith, Z.G., and Dhanasekaran, D.N. (2007). G protein regulation of MAPK networks. Oncogene *26*, 3122–3142.

75. Ferrández-Roldán, A., Fabregà-Torrus, M., Sánchez-Serna, G., Duran-Bello, E., Joaquín-Lluís, M., Bujosa, P., Plana-Carmona, M., Garcia-Fernàndez, J., Albalat, R., and Cañestro, C. (2021). Cardiopharyngeal deconstruction and ancestral tunicate sessility. Nature *599*, 431–435.

76. Nanglu, K., Lerosey-Aubril, R., Weaver, J.C., and Ortega-Hernández, J. (2023). A mid-Cambrian tunicate and the deep origin of the ascidiacean body plan. Nat. Commun. *14*, 3832.

77. Ryan, K., and Meinertzhagen, I.A. (2019). Neuronal identity: the neuron types of a simple chordate sibling, the tadpole larva of Ciona intestinalis. Curr. Opin. Neurobiol. *56*, 47–60.

78. Ben-Ari, Y., Gaiarsa, J.-L., Tyzio, R., and Khazipov, R. (2007). GABA: a pioneer transmitter that excites immature neurons and generates primitive oscillations.

Physiol. Rev. *87*, 1215–1284.

79. Pfeil, E.M., Brands, J., Merten, N., Vögtle, T., Vescovo, M., Rick, U., Albrecht, I.-M., Heycke, N., Kawakami, K., Ono, Y., et al. (2020). Heterotrimeric G protein subunit Gαq is a master switch for Gβγ-mediated calcium mobilization by GI-coupled GPCRs. Mol. Cells. 10.2139/ssrn.3578140.

80. Azevedo, M.F., Faucz, F.R., Bimpaki, E., Horvath, A., Levy, I., de Alexandre, R.B., Ahmad, F., Manganiello, V., and Stratakis, C.A. (2014). Clinical and molecular genetics of the phosphodiesterases (PDEs). Endocr. Rev. *35*, 195–233.

81. Menegaz, D., Hagan, D.W., Almaça, J., Cianciaruso, C., Rodriguez-Diaz, R., Molina, J., Dolan, R.M., Becker, M.W., Schwalie, P.C., Nano, R., et al. (2019). Mechanism and effects of pulsatile GABA secretion from cytosolic pools in the human beta cell. Nat Metab *1*, 1110–1126.

82. Wagner, E., Stolfi, A., Gi Choi, Y., and Levine, M. (2014). Islet is a key determinant of ascidian palp morphogenesis. Development *141*, 3084–3092.

83. Kusakabe, T.G., Sakai, T., Aoyama, M., Kitajima, Y., Miyamoto, Y., Takigawa, T., Daido, Y., Fujiwara, K., Terashima, Y., Sugiuchi, Y., et al. (2012). A conserved non-reproductive GnRH system in chordates. PLoS One *7*, e41955.

84. Tello, J.A., Rivier, J.E., and Sherwood, N.M. (2005). Tunicate gonadotropin-releasing hormone (GnRH) peptides selectively activate Ciona intestinalis GnRH receptors and the green monkey type II GnRH receptor. Endocrinology *146*, 4061–4073.

85. Sakai, T., Yamamoto, T., Matsubara, S., Kawada, T., and Satake, H. (2020). Invertebrate Gonadotropin-Releasing Hormone Receptor Signaling and Its Relevant Biological Actions. Int. J. Mol. Sci. *21*. 10.3390/ijms21228544.

86. Jackson, D., Leys, S.P., Hinman, V.F., Woods, R., Lavin, M.F., and Degnan, B.M. (2002). Ecological regulation of development: induction of marine invertebrate metamorphosis. Int. J. Dev. Biol. *46*, 679–686.

87. Lagersson, N., and Høeg, J. (2002). Settlement behavior and antennulary biomechanics in cypris larvae of Balanus amphitrite (Crustacea: Thecostraca: Cirripedia). Mar. Biol. *141*, 513–526.

88. Morse, D., Hooker, N., and Duncan, H. (1980). GABA induces metamorphosis in Haliotis, V: Stereochemical specificity. Brain Res. Bull. *5*, 381–387.

89. Rahmani, M., and Ueharai, T. (2001). Induction of metamorphosis and substratum preference in four sympatric and closely related species of sea urchins (genus Echinometra) in Okinawa. Zool. Stud. *40*, 29–43.

90. Pearce, C.M., and Scheibling, R.E. (1990). Induction of metamorphosis of larvae of the Green Sea urchin, Strongylocentrotus droebachiensis, by coralline red algae. Biol. Bull. *179*, 304–311.

91. Leitz, T., and Müller, W.A. (1987). Evidence for the involvement of PI-signaling and diacylglycerol second messengers in the initiation of metamorphosis in the hydroid Hydractinia echinata Fleming. Dev. Biol. *121*, 82–89.

92. Rittschof, D., Maki, J., Mitchell, R., and Costlow, J.D. (1986). Ion and neuropharmacological studies of barnacle settlement. Neth. J. Sea Res. *20*, 269–275.

93. Clare, A.S. (1996). Signal transduction in barnacle settlement: Calcium re-visited. Biofouling *10*, 141–159.

94. Holm, E., Nedved, B., Carpizo-Ituarte, E., and Hadfield, M. (1998). Metamorphic-Signal Transduction in Hydroides elegans (Polychaeta: Serpulidae) Is Not Mediated by a G Protein. Biol. Bull. *195*, 21–29.

95. Roure, A., Rothbächer, U., Robin, F., Kalmar, E., Ferone, G., Lamy, C., Missero, C., Mueller, F., and Lemaire, P. (2007). A multicassette Gateway vector set for high throughput and comparative analyses in ciona and vertebrate embryos. PLoS One *2*, e916.

96. Hozumi, A., Kawai, N., Yoshida, R., Ogura, Y., Ohta, N., Satake, H., Satoh, N., and Sasakura, Y. (2010). Efficient transposition of a single Minos transposon copy in the genome of the ascidian Ciona intestinalis with a transgenic line expressing transposase in eggs. Dev. Dyn. *239*, 1076–1088.

97. Akanuma, T., Hori, S., Darras, S., and Nishida, H. (2002). Notch signaling is involved in nervous system formation in ascidian embryos. Dev. Genes Evol. *212*, 459–472.

98. Sasakura, Y., Suzuki, M.M., Hozumi, A., Inaba, K., and Satoh, N. (2010). Maternal factor-mediated epigenetic gene silencing in the ascidian Ciona intestinalis. Mol. Genet. Genomics *283*, 99–110.

99. Kobayashi, K., and Satou, Y. (2018). Microinjection of exogenous nucleic acids into eggs: Ciona species. Adv. Exp. Med. Biol. *1029*, 5–13.

100. Satou, Y., Imai, K.S., and Satoh, N. (2001). Action of morpholinos in Ciona embryos. Genesis *30*, 103–106.

101. Altschul, S.F., Madden, T.L., Schäffer, A.A., Zhang, J., Zhang, Z., Miller, W., and Lipman, D.J. (1997). Gapped BLAST and PSI-BLAST: a new generation of protein database search programs. Nucleic Acids Res. *25*, 3389–3402.

102. Notredame, C., Higgins, D.G., and Heringa, J. (2000). T-Coffee: A novel method for fast and accurate multiple sequence alignment. J. Mol. Biol. *302*, 205–217.

103. Wallace, I.M., O'Sullivan, O., Higgins, D.G., and Notredame, C. (2006). M-Coffee: combining multiple sequence alignment methods with T-Coffee. Nucleic Acids Res. *34*, 1692–1699.

104. Tamura, K., Stecher, G., and Kumar, S. (2021). MEGA11: Molecular Evolutionary Genetics Analysis version 11. Mol. Biol. Evol. *38*, 3022–3027.

105. Whelan, S., and Goldman, N. (2001). A general empirical model of protein evolution derived from multiple protein families using a maximum-likelihood approach. Mol. Biol. Evol. *18*, 691–699.

Figure legends

Figure 1. Gq and Gs pathways are required for *Ciona* metamorphosis.

(A) Schematic illustration of *Ciona* metamorphosis.

(B) A larva knocked down with *Gαq* using the antisense morpholino oligonucleotide (MO). Metamorphosis did not initiate at 2 days post-fertilization (2 dpf).

(C) A *Gαs* knockdown larva.

(D) A control animal injected with the standard (STD) MO. Metamorphosis initiated, as indicated by the completion of tail regression.

(E) Effect of *Gαq* knockdown on the percentage of metamorphosis initiation (indicated by the initiation of tail regression), shown as box-and-whisker plots. Dots indicate experiment replicates. ***, $p<0.001$ (Fisher's exact test). n, number of examined larvae in total.

(F) Effect of *Gαs* knockdown.

(G-I) Effects of *PLCβ1/2/3*, *PLCβ4*, and *IP3R* knockdowns.

(J-M) Results of the experiments where adhesion was prevented by tail amputation and laying larvae on agar-coated plates.

(J) A control larva overexpressing the *Kaede* reporter in the entire nervous system using the *PC2 cis* element.

(K) A larva overexpressing constitutive active (ca)*PLCβ1/2/3*.

(L) Effect of ca*Gαq* overexpression.

(M) Effect of ca*PLCβ1/2/3* overexpression.

(N-O) Live imaging of Ca^{2+} transient, monitored by injecting *GCaMP8* mRNA.

(N) Snapshot of the control larva injected with *GCaMP8* mRNA. An increase in the fluorescence intensity in the adhesive papillae (arrow) was observed. Rod, the position of the glass rod used to stimulate papillae. The percentage and number exhibit the rate of animals showing Ca^{2+} transient in the papillae.

(O) A larva injected with *Gαq* MO plus *GCaMP8* mRNA. An increase in the fluorescence intensity in the papillae (arrow) was not observed even though the brightness of the whole body was raised. See also Figure S1.

Figure 2. cAMP initiates *Ciona* metamorphosis.

(A) An adhesion-prevented control (uninjected) larva at 2 dpf. Metamorphosis did not initiate.

(B) An animal with adhesion prevention and overexpression of ca*Gαs* in the entire nervous system. Metamorphosis initiated.

(C) Effect of ca*Gαs* overexpression.

(D) A control (uninjected) larva.

(E) A theophylline-treated animal. Metamorphosis initiated.

(F) Effect of theophylline treatment.

(G) Effect of *bPAC* overexpression in the nervous system.

(H) Effect of *bPAC* overexpression over time. In this experiment, adhesion was permitted. Control groups (overexpressed with mCherry) exhibited a slower initiation of metamorphosis than bPAC-overexpressed groups.

Figure 3. Gq and Gs pathways are activated in the adhesive papillae to initiate metamorphosis.

(A) A theophylline-treated animal. Metamorphosis initiated.

(B) A papilla-amputated larva treated with theophylline. Metamorphosis did not initiate.

(C) Effect of papilla amputation on theophylline treatment.

(D) Effects of papilla amputation on ca*Gαq*, ca*PLCβ1/2/3*, ca*Gαs*, and bPAC overexpression.

(E) Measurement of cAMP concentration, as indicated by the fluorescence of Pink Flamindo. Left, the quantification of Pink Flamindo fluorescent intensity is shown for a

larva that initiated metamorphosis at the time indicated by an arrowhead. The time of stimulation of the adhesive papillae with a glass rod is denoted by a bar. Right, the position of the region of interest (ROI). See also Figure S3.

Figure 4. Relationships between Gq and Gs pathways in metamorphosis.

(A) A *Gαq* knockdown larva.

(B) Theophylline ameliorated the effect of *Gαq* knockdown.

(C) Effect of theophylline on *Gαq* knockdown.

(D) Effect of theophylline on *PLCβ* knockdown. In this experiment, *PLCβ1/2/3* and *PLCβ4* were knocked down simultaneously.

(E) Effect of theophylline on *IP3R* knockdown.

(F) Effect of ca*Gαs* overexpression on *Gαq* knockdown.

(G) *Gαs* is not necessary for Ca^{2+} transient in the adhesive papillae (arrow) upon adhesion.

(H) A *Gαq* knockdown and *Kaede*-overexpressed larva.

(I) A *Gαq* knockdown and ca*PLCβ1/2/3*-overexpressed larva.

(J) A *Gαs* knockdown and ca*PLCβ1/2/3*-overexpressed larva.

(K) Effect of ca*PLCβ1/2/3* overexpression on *Gαq* knockdown.

(L) Effect of ca*PLCβ1/2/3* overexpression on *Gαs* knockdown.

(M) Effect of ca*Gαq* overexpression on *Gαs* knockdown.

(N) Effect of theophylline treatment on *Gαs* knockdown.

Figure 5. GABA functions in the adhesive papillae to induce metamorphosis.

(A) A *GABABR1* knockdown and *mCherry*-overexpressed larva.

(B) A *GABABR1* knockdown and ca*PLCβ1/2/3*-overexpressed larva. Metamorphosis initiated.

(C) Effect of ca*PLCβ1/2/3* overexpression on *GABABR1* knockdown.

(D) Effect of theophylline on *GABABR1* and *GAD* knockdowns.

(E) GABA is necessary for Ca^{2+} transient in the adhesive papillae (arrow).

(F) Effect of GABA on *Gαq* knockdown.

(G) Effect of GABA on *PLCβ* knockdown.

(H) Effect of GABA on *Gαs* knockdown. See also Figure S4.

Figure 6. Gi is required for metamorphosis initiation.

(A) Effect of *Gαi* knockdown.

(B) A control animal injected with STD MO.

(C) A *dvGαi_Chr2* knockdown larva.

(D) A *dvGαi_Chr2* knockdown and theophylline-treated animal.

(E) Effects of GABA and theophylline on *dvGαi_Chr2* knockdown.

(F) Effects of wt*Gαi* and wt*Gαs* overexpression.

(G) Effect of dn*Gαi* overexpression.

(H) Effect of *GABABR1* and *Gαq* simultaneous knockdown.

(I) Effects of ca*PLCβ1/2/3* and ca*Gαs* overexpressions on *GABABR1* and *Gαq* simultaneous knockdown.

(J) *GIRK* knockdown promoted metamorphosis initiation.

(K) Effect of U0126 on GABA treatment.

(L) Effect of U0126 on theophylline treatment. See also Figure S5.

Figure 7. Schematic illustration of the signaling cascades for initiating *Ciona* metamorphosis. AC, adenylate cyclase; ER, endoplasmic reticulum; GPCR, G-protein coupled receptor; PKA, protein kinase A.

FIGURE LEGENDS for SUPPLEMENTARY FIGURES

Supplementary Figure S1. ***Ciona* phospholipase β proteins**

Phylogenetic relationships between PLCβ proteins, as revealed by the maximum likelihood method. The number beside each branch indicates the percentage of times that a node was supported in 1,000 bootstrap pseudoreplications. Scores equal to or exceeding 50% are shown. *Ciona* PLCβs are indicated by black circles. Human homologs are indicated by accession numbers in the Uniprot database (https://www.uniprot.org) and "HS" for *Homo sapiens*.

Supplementary Figure S2. *Ciona* phosphodiesterase repertoire

(A) Phylogenetic relationships between PDEs. Black circles and gene models indicate *Ciona* protein models in the Ghost database (http://ghost.zool.kyoto-u.ac.jp/default_ht.html). The numbers and letters in parentheses indicate the PDE groups and their suspected substrates. A, cAMP; G, cGMP; D, dual substrate. Human and insect proteins are shown by Uniprot (https://www.uniprot.org) accession numbers, as well as "HS" for *Homo sapiens* and "DM" for *Drosophila melanogaster* proteins.
(B) Expression profiles of the genes related to Gq and Gs pathways, as revealed by RNA-seq of the papilla region. RPKM, reads per kilobase of exon per million mapped reads. See also Table S1.

Supplementary Figure S3. cAMP increase in the papillae is coupled with metamorphosis initiation

Measurement of cAMP concentration in the larva that did not initiate metamorphosis upon stimulation of the papillae, as indicated by the fluorescence of Pink Flamindo.

Left, the quantification of Pink Flamindo fluorescent intensity of a larva that did not initiate metamorphosis; right, the position of the region of interest (ROI).

Supplementary Figure S4. GABA stimulates the adhesive papillae to initiate metamorphosis.

(A) A GABA-treated animal initiated metamorphosis.

(B) A papilla-amputated larva treated with GABA. Metamorphosis was not initiated.

(C) Effect of papilla amputation on GABA treatment.

(D-H) The sensory vesicle is not required for the anterior region to respond to GABA.

(D) Schematic of the experiment.

(E) A control anterior fragment at 2 dpf.

(F) Anterior fragment treated with GABA. The percentage indicates the proportion of the fragments exhibiting the morphological signature of metamorphosis.

(G) Anterior fragment treated with theophylline.

(H) Expression levels of two GABA-responsive genes in the control- and GABA-treated anterior fragments, as revealed by quantitative RT-PCR.

Supplementary Figure S5. *Ciona* has atypical Gαi proteins.

(A) Phylogenetic relationships between Gα proteins, as revealed by the maximum likelihood method. The three atypical Gα proteins are highlighted in red.

(B) Comparison of the five C-terminal amino acid sequences of Gα proteins that are shown to be essential for their functions, including two additional amino acids for dvGαi_Chr2. Residues conserved with human Gαi1 are shown in red.

Supplementary Figure S6. Autonomous activity of wild-type Gαq.

(A) Effect of wt*Gαq* overexpression in the adhesion-permitted condition.

(B) Effect of wt*Gαq* overexpression in the adhesion-prevented condition.

(C) Effect of wt*Gαq* overexpression on *Gαs* knockdown.

(D) Morphology of ca*Gαq*-overexpressed larva at 1 dpf (before initiation of metamorphosis).

(E) Morphology of wt*Gαq*-overexpressed larva at 1 dpf.

(F) Effect of dn*Gαq* overexpression in the adhesion-permitted condition.

Hozumi et al., Figure 1

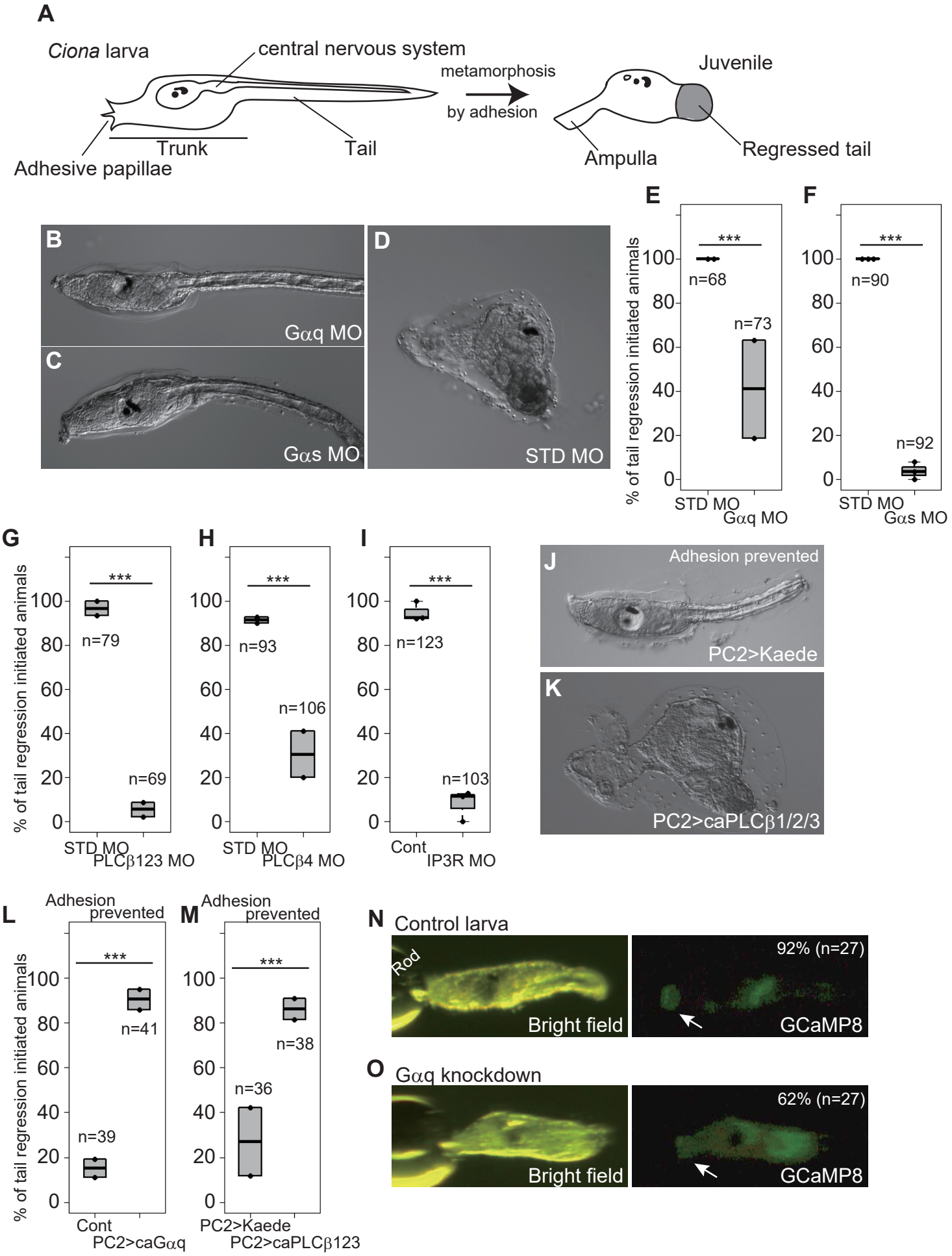

Hozumi et al., Figure 2

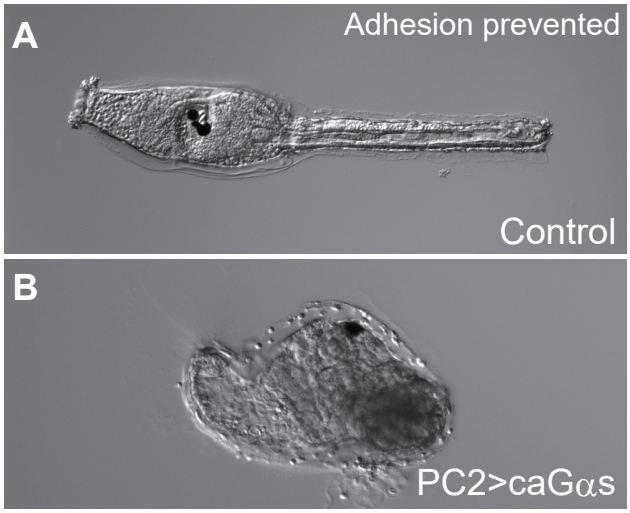

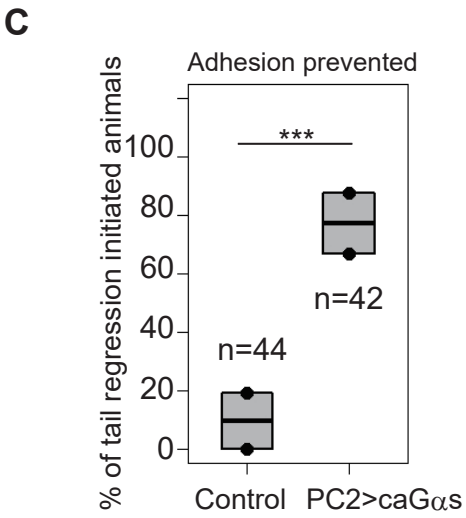

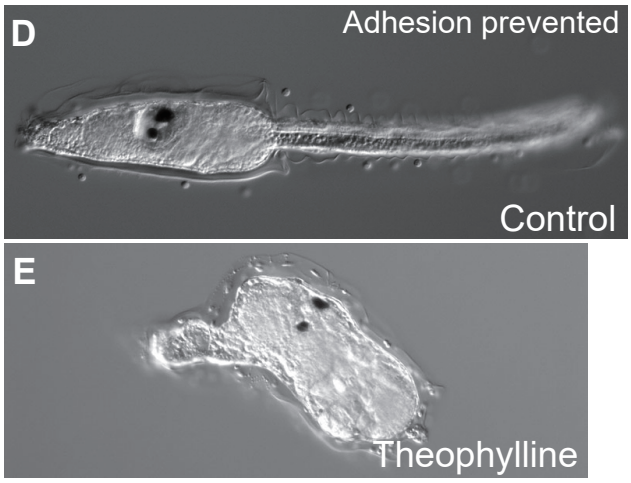

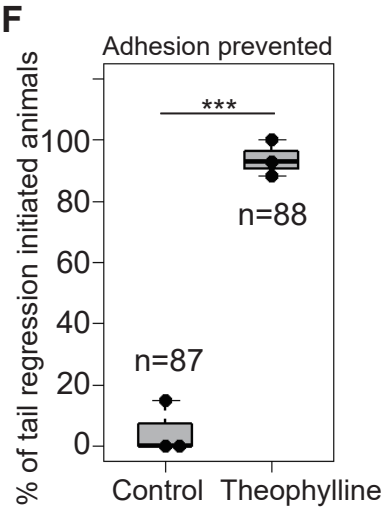

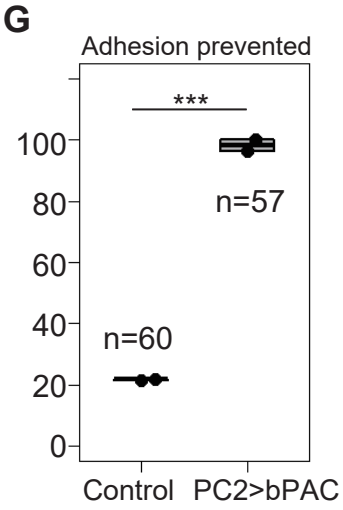

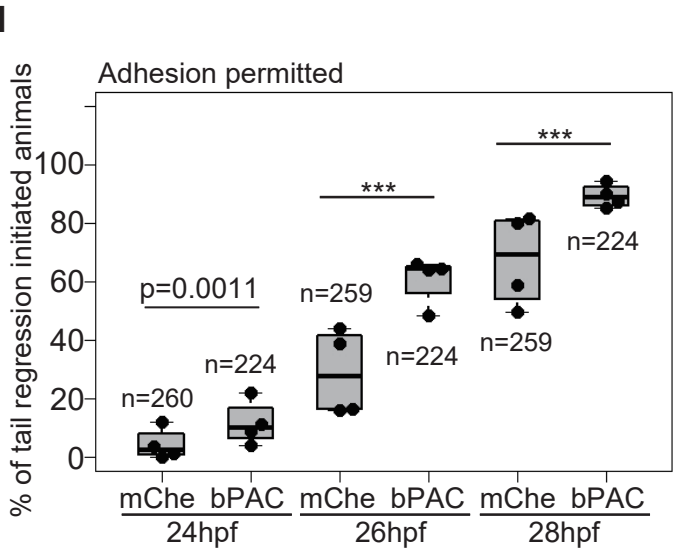

Hozumi et al., Figure 3

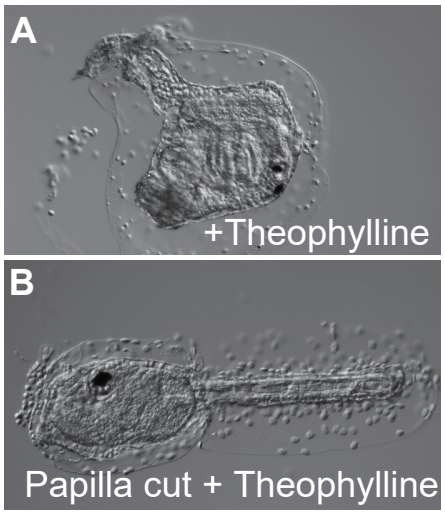

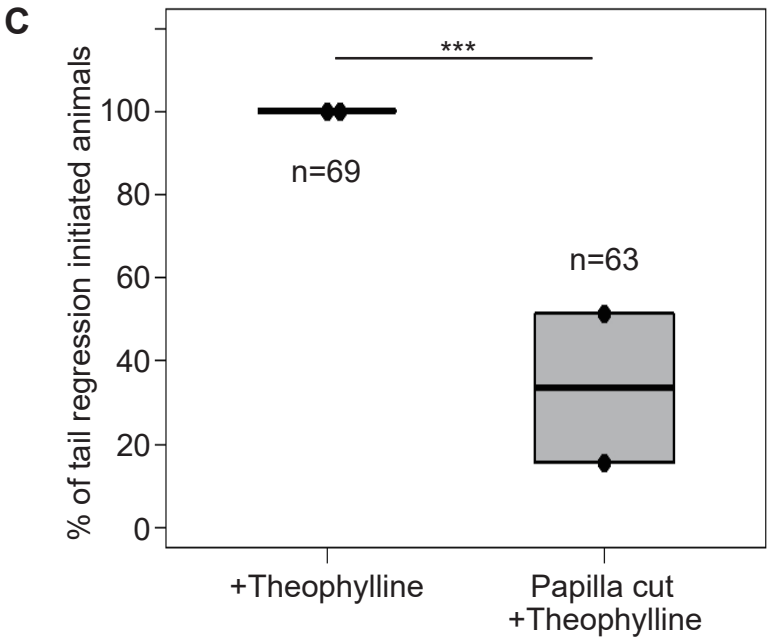

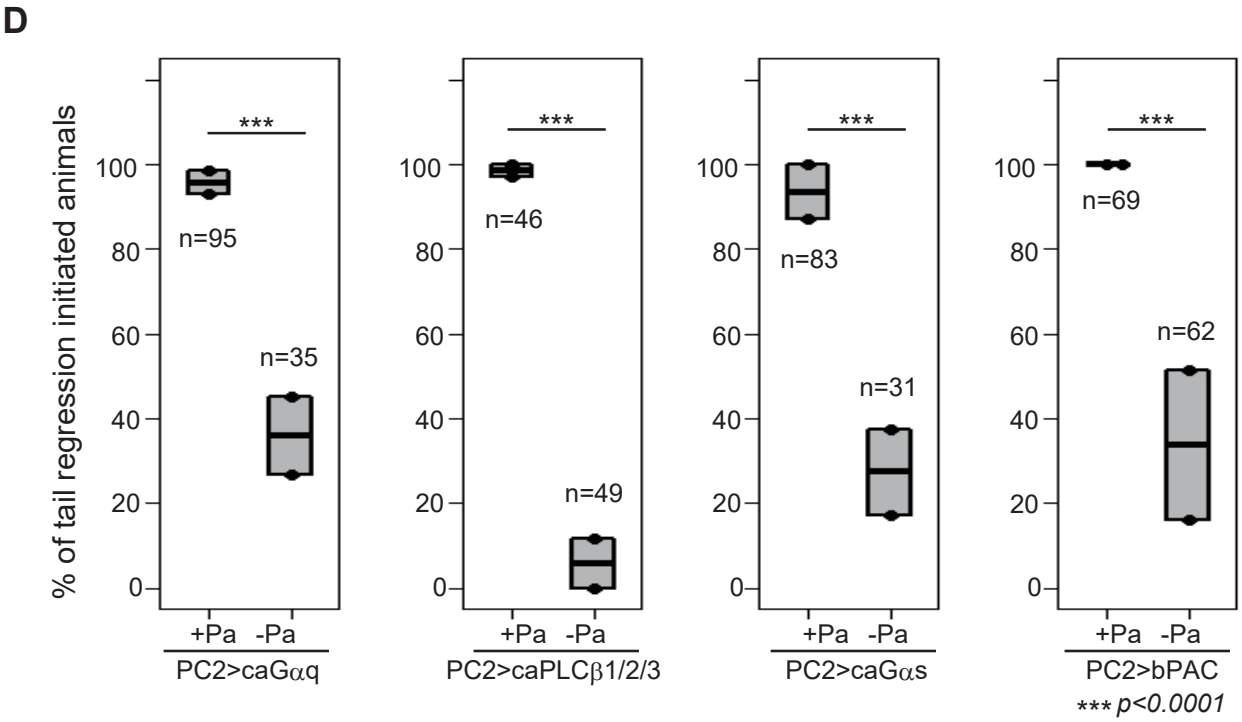

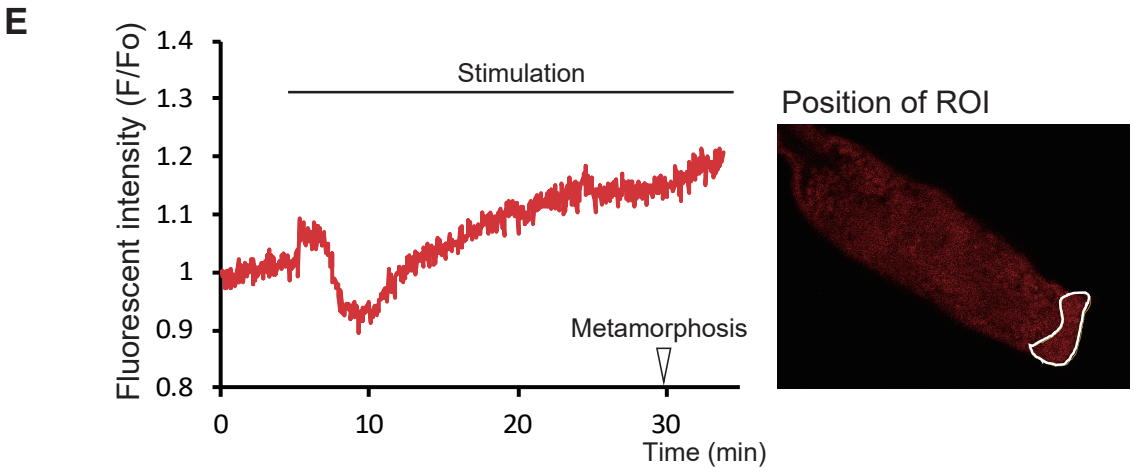

Hozumi et al., Figure 4

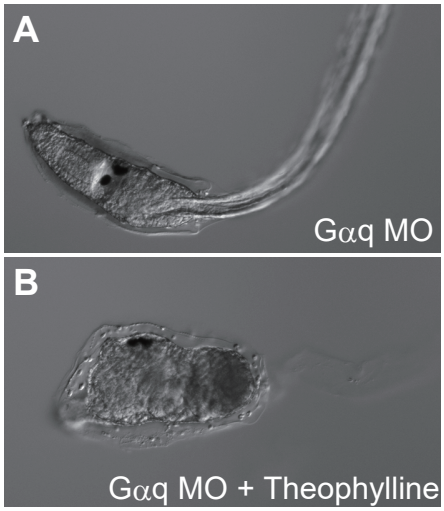

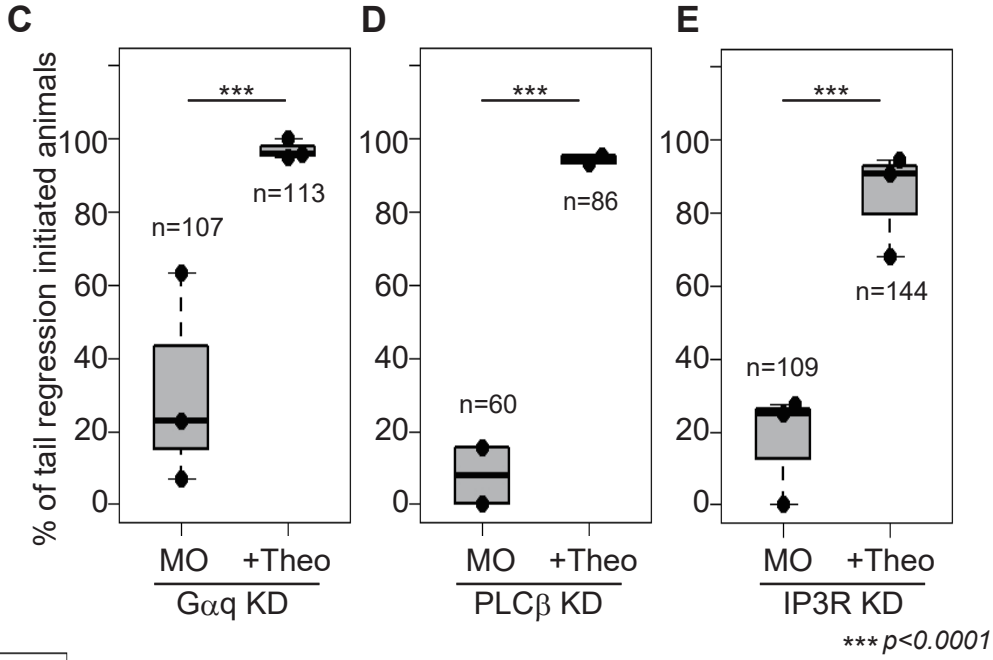

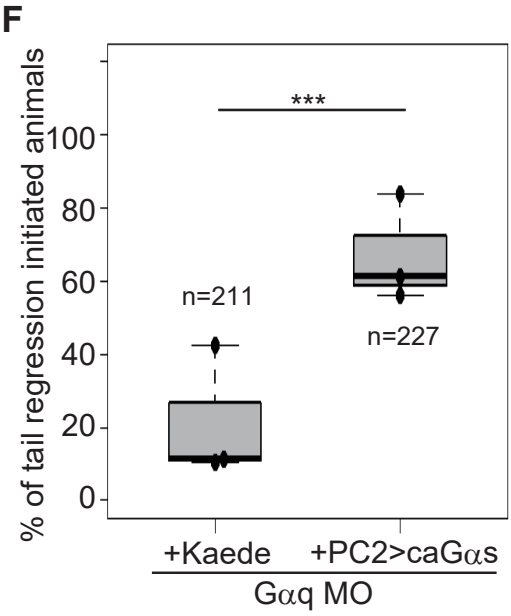

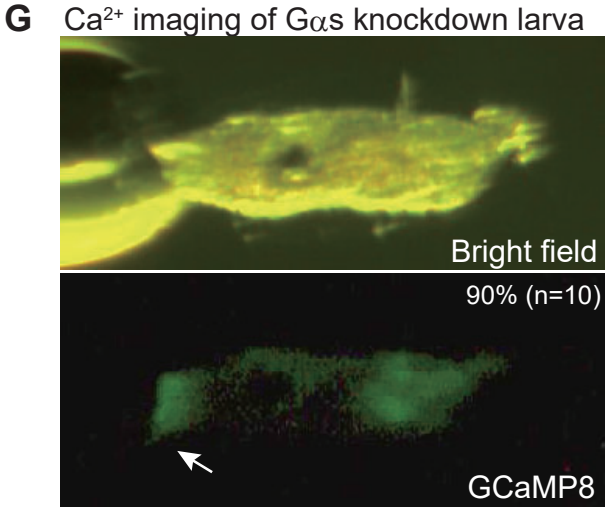

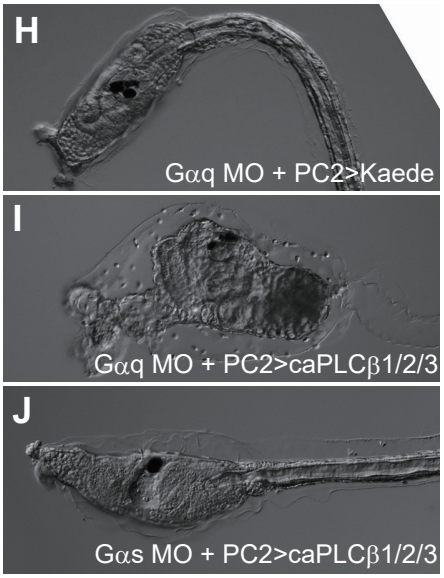

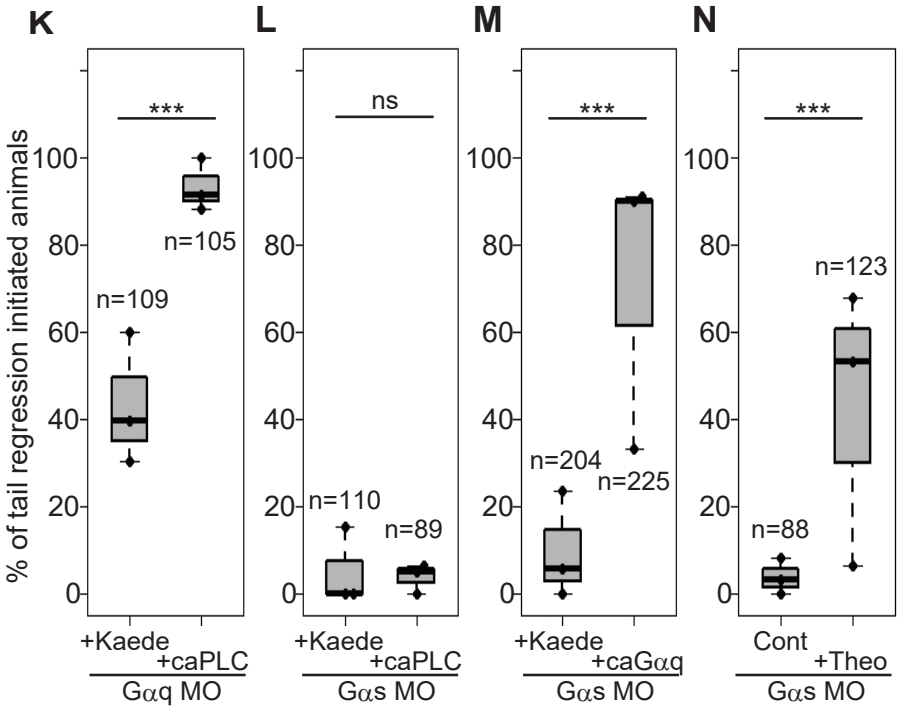

Hozumi et al., Figure 5

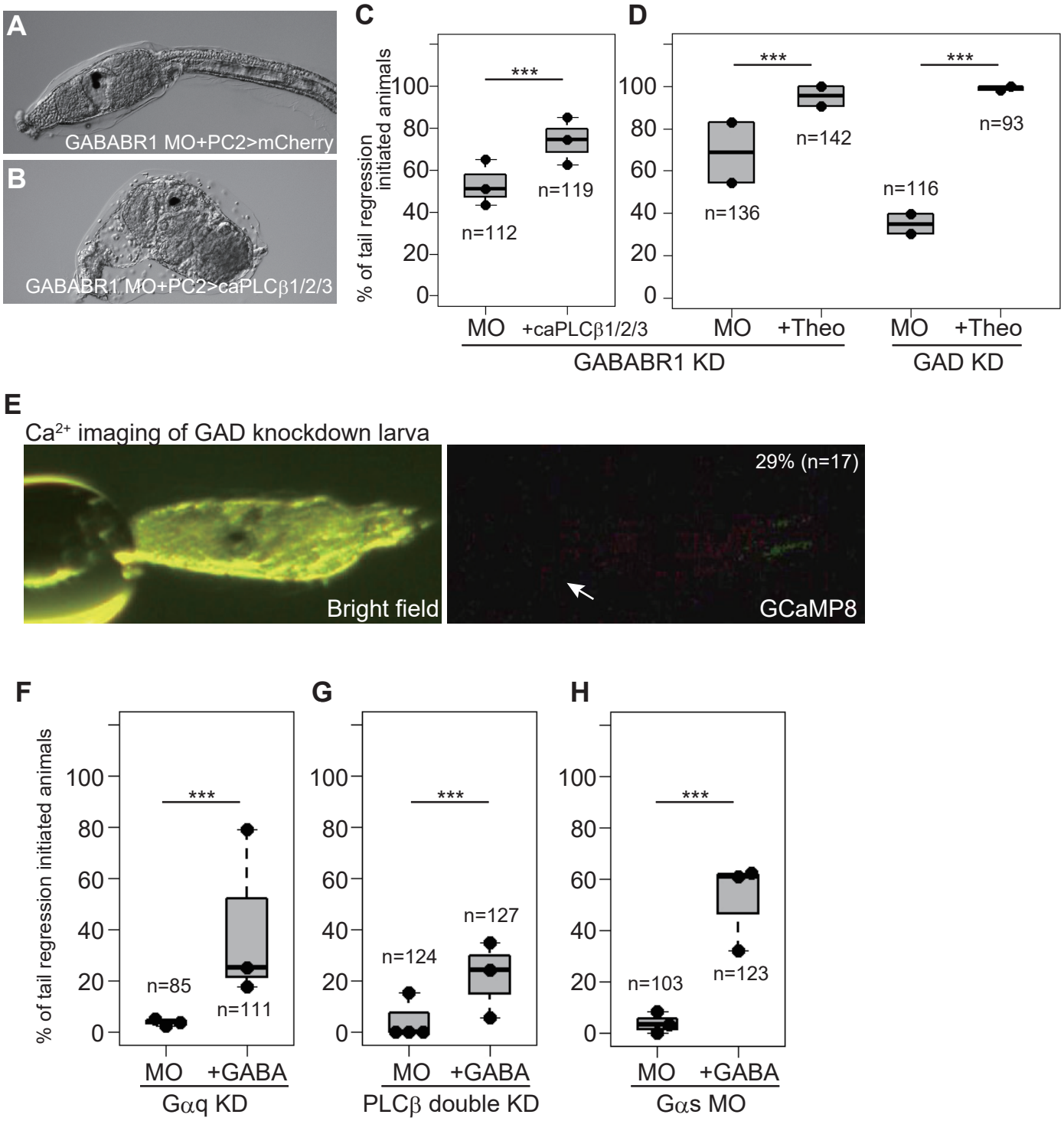

Hozumi et al., Figure 6

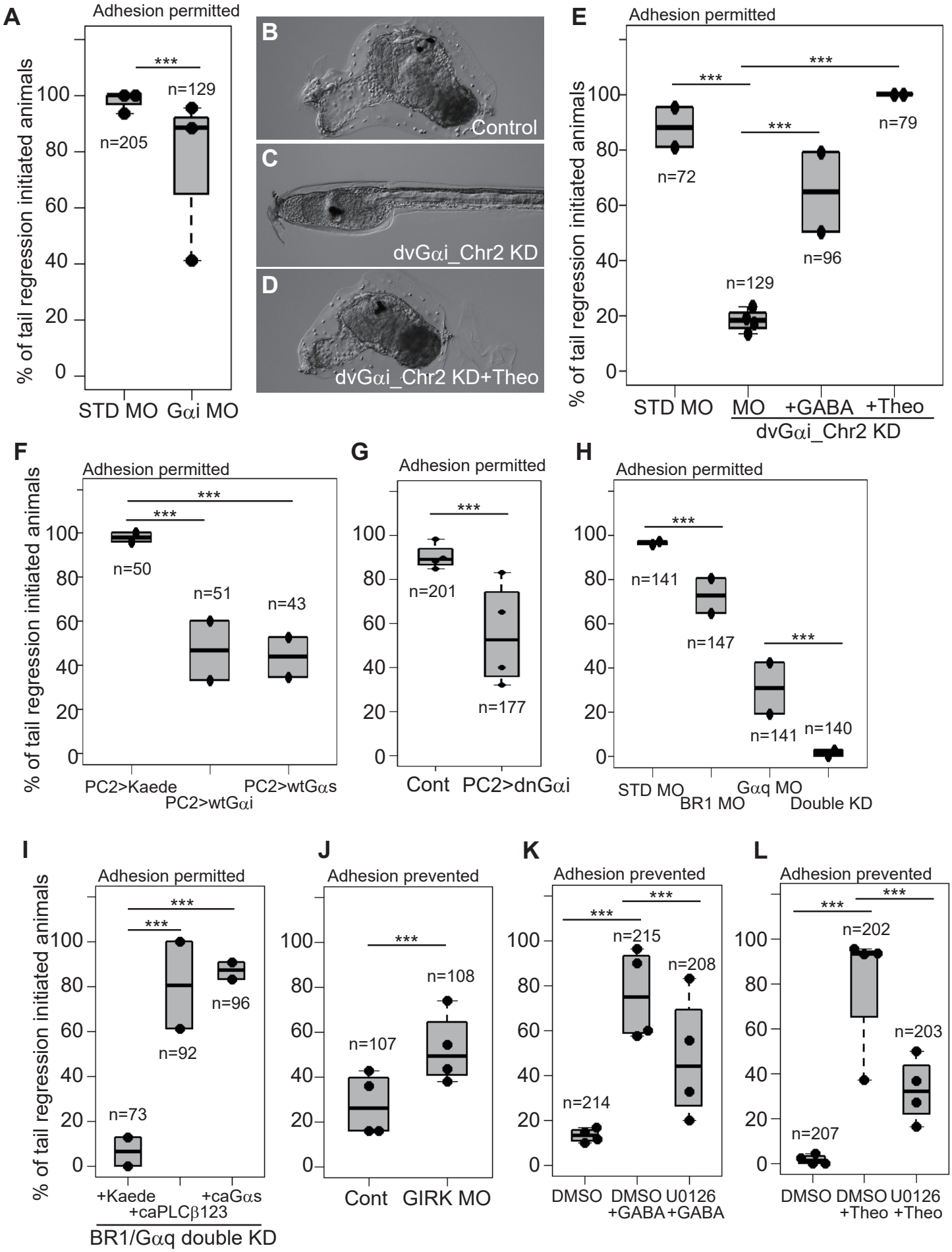

Hozumi et al., Figure 7

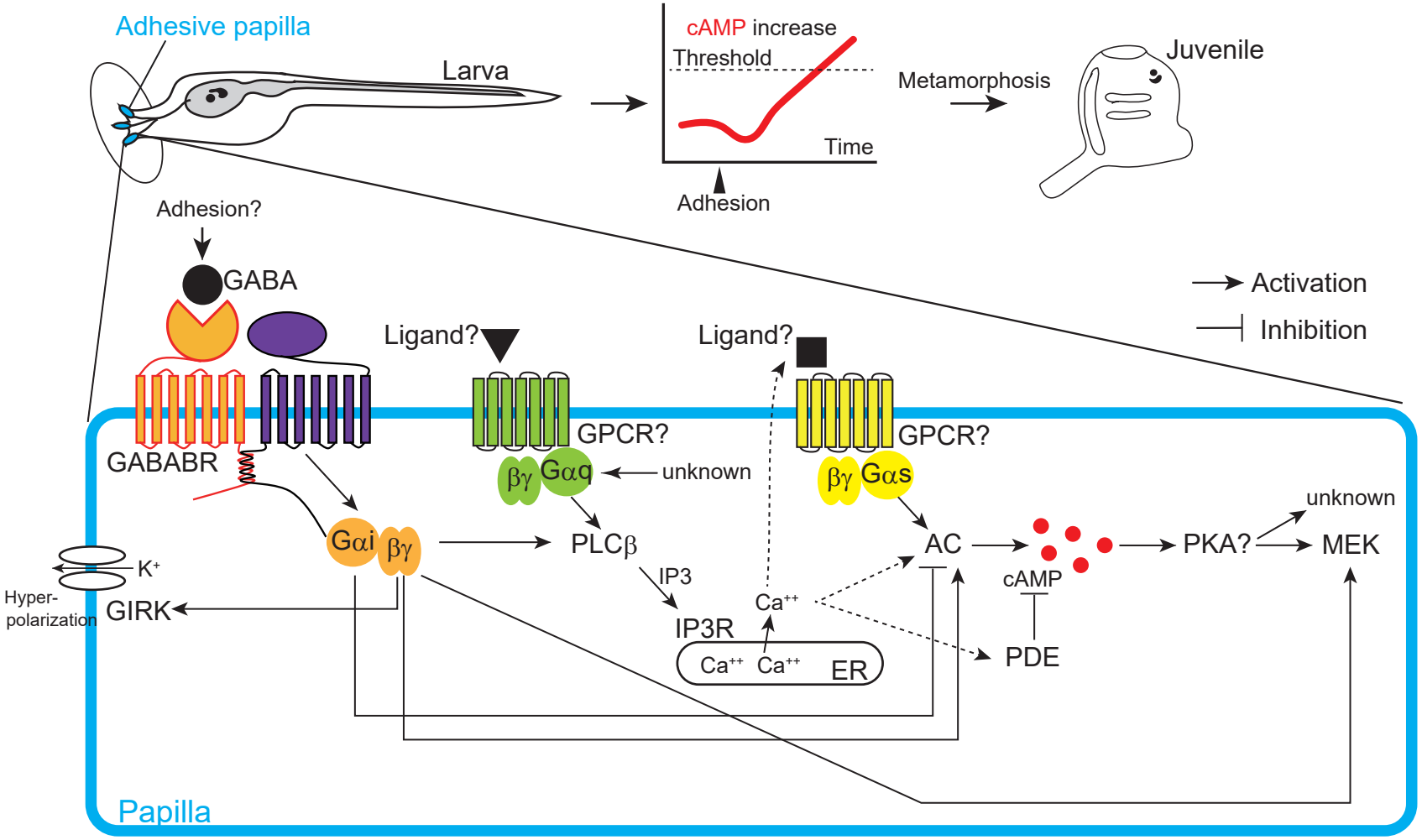

Hozumi et al. Supplementary Figure S1

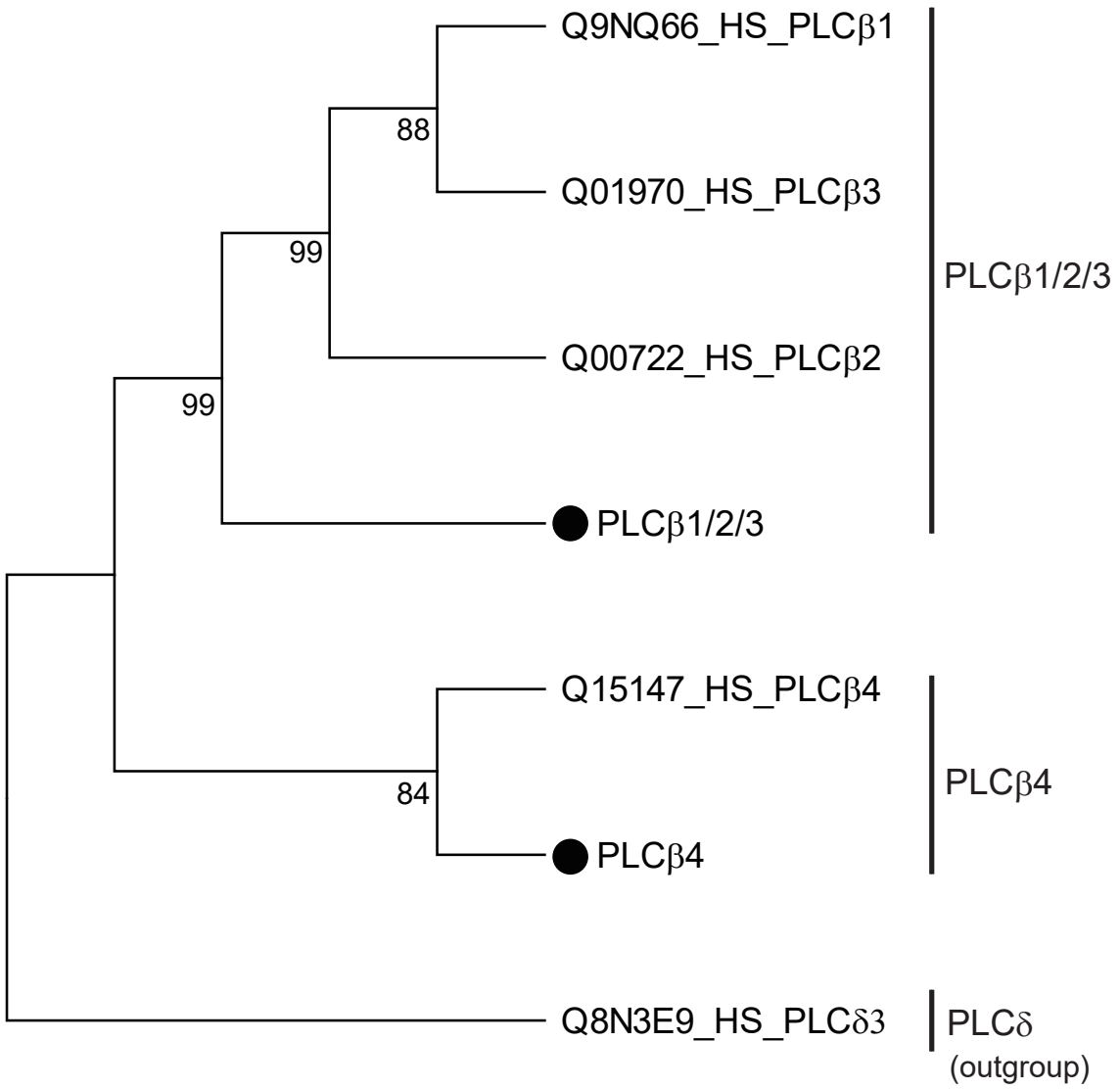

Hozumi et al. Supplementary Figure S2

A

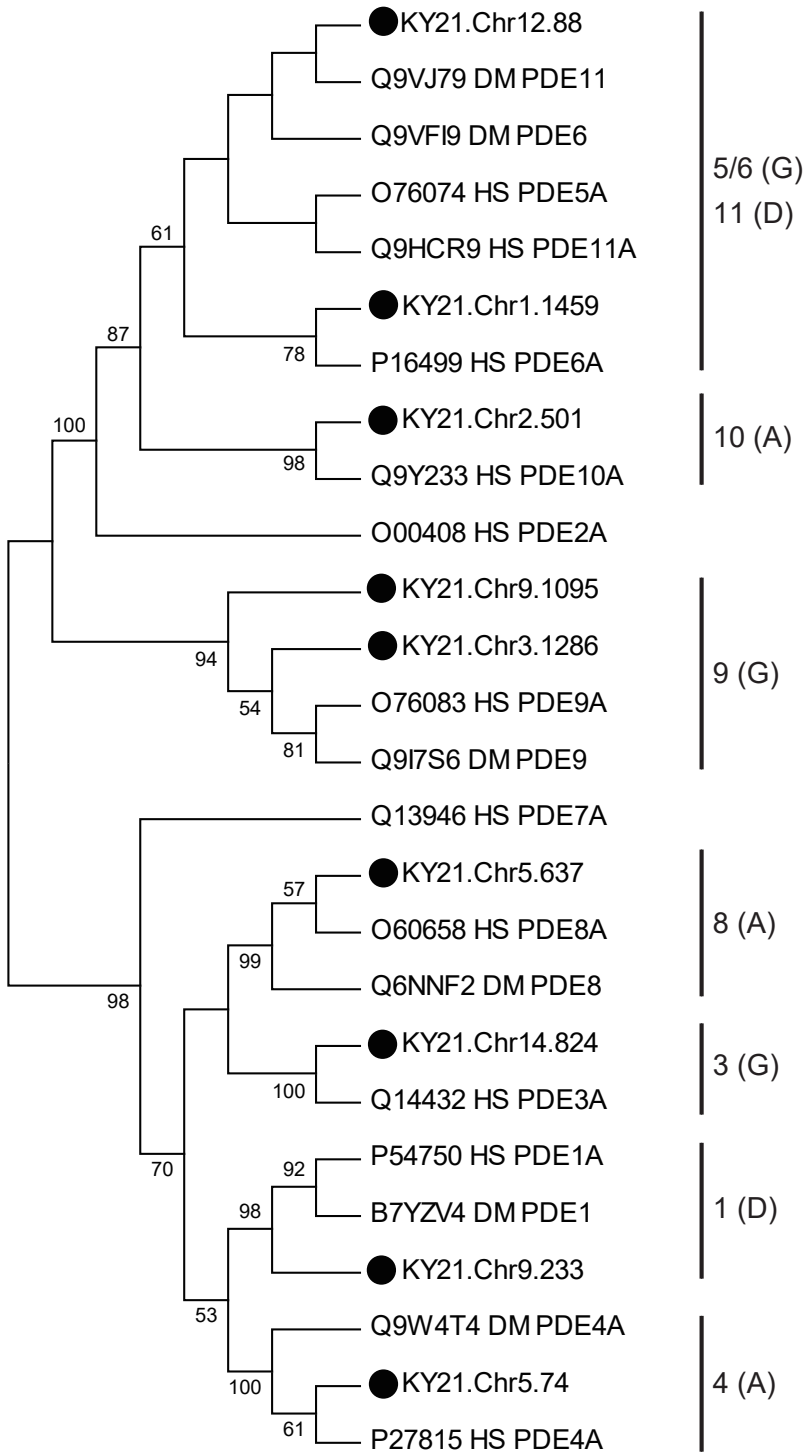

B

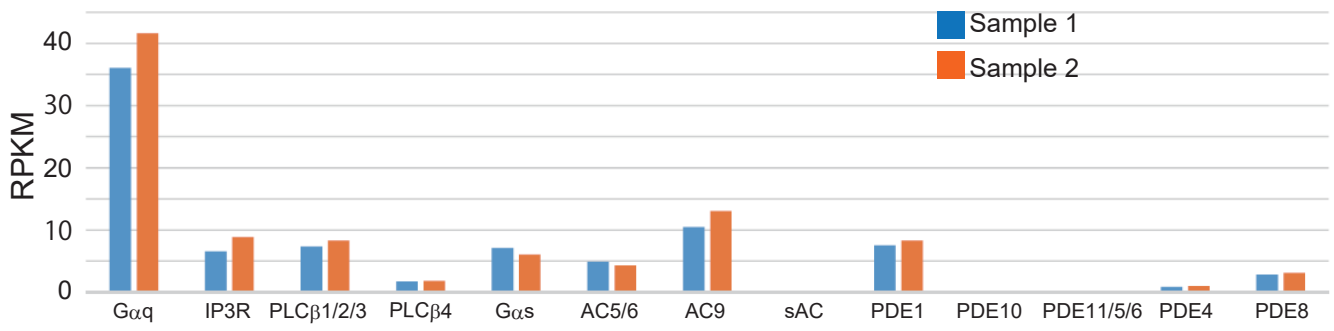

Hozumi et al., Supplementary Figure S3

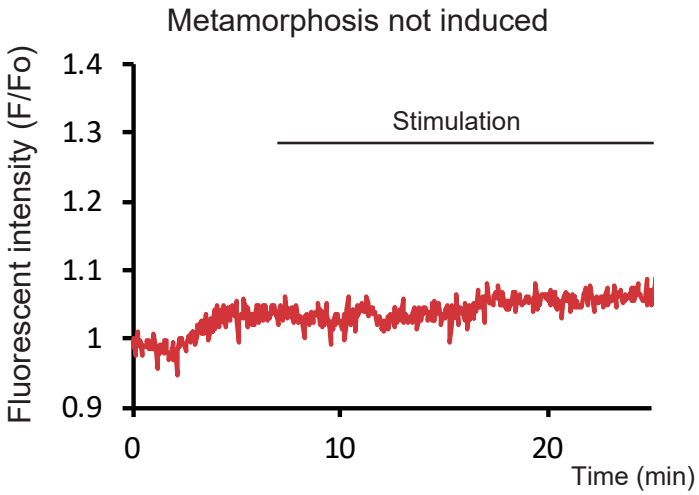

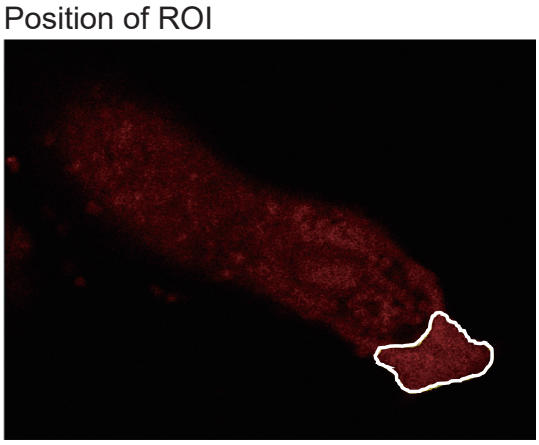

Hozumi et al., Supplementary Figure S4

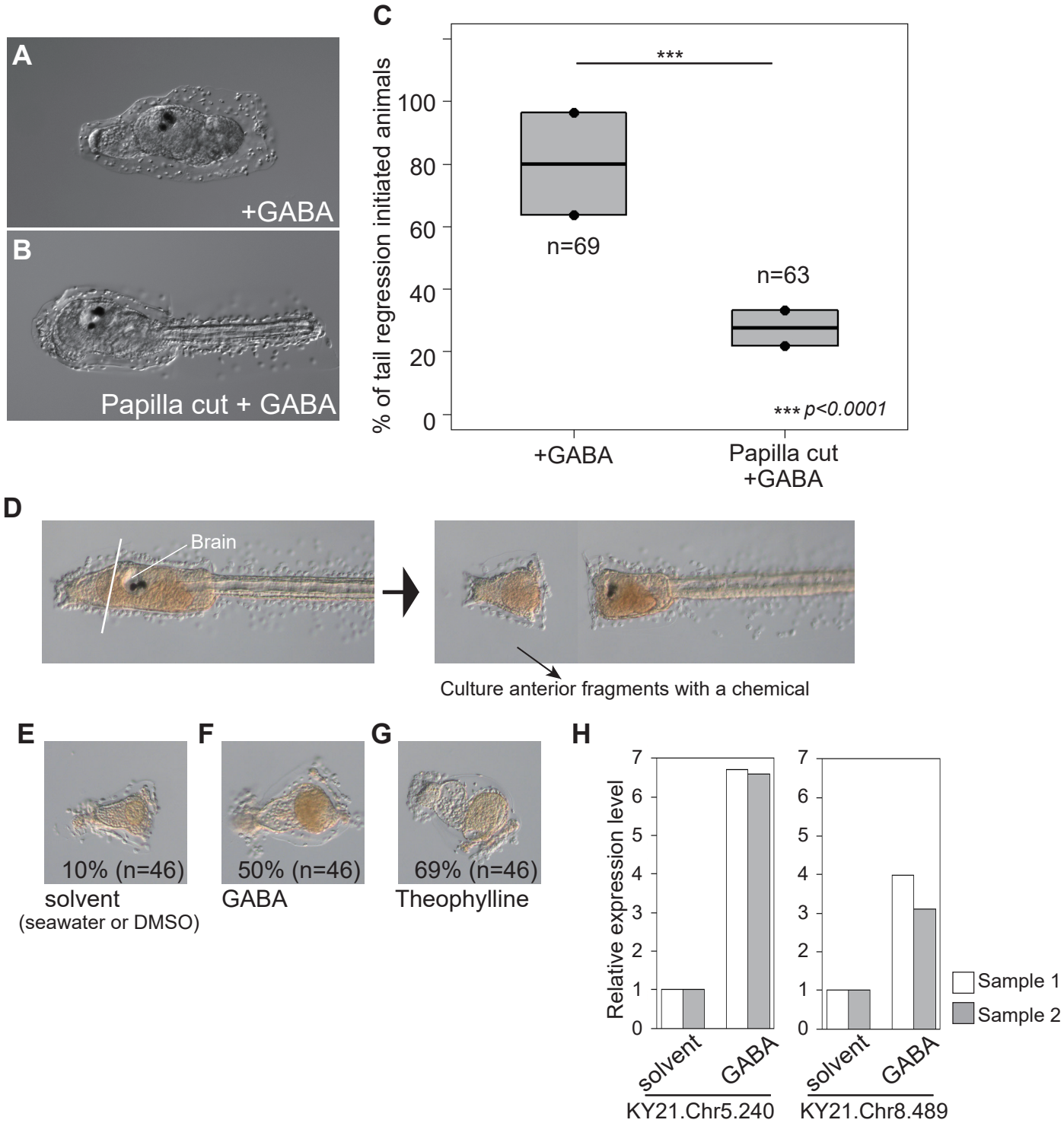

Hozumi et al., Supplementary Figure S5

A

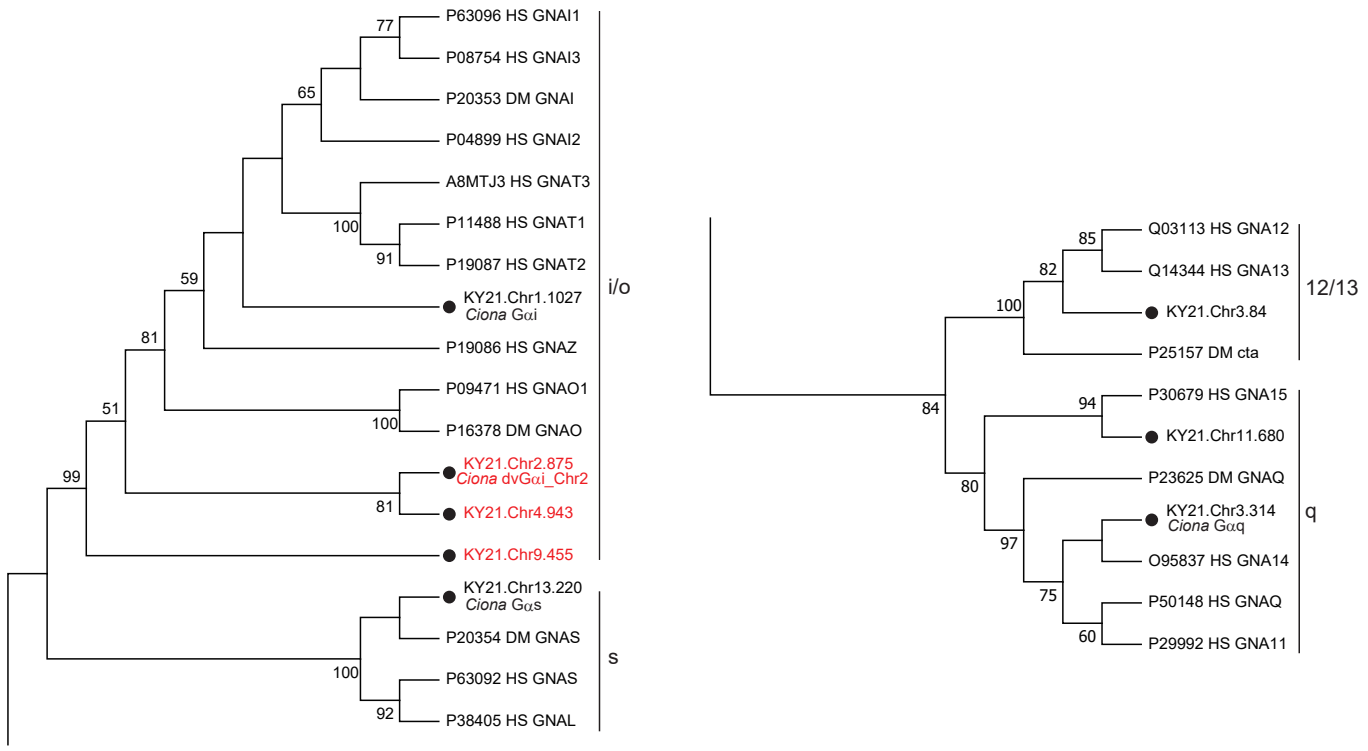

B

		Residue from the C-terminus						
		-5	-4	-3	-2	-1		
Ciona	Gαq	E	Y	N	**L**	V		
	Gαs	Q	Y	E	**L**	L		
	Gαi	**D**	**C**	**G**	**L**	**F**		
	dvGαi_Chr2	**D**	L	**G**	**L**	M	T	E
Human	Gαq	E	Y	N	**L**	V		
	Gαs	Q	Y	E	**L**	L		
	Gαi1	**D**	**C**	**G**	**L**	**F**		
	Gαi2	**D**	**C**	**G**	**L**	**F**		
	Gαi3	E	**C**	**G**	**L**	Y		
	Gαo	G	**C**	**G**	**L**	Y		
	Gα12	**D**	I	M	**L**	Q		
	Gα13	Q	L	M	**L**	Q		

Hozumi et al., Supplementary Figure S6

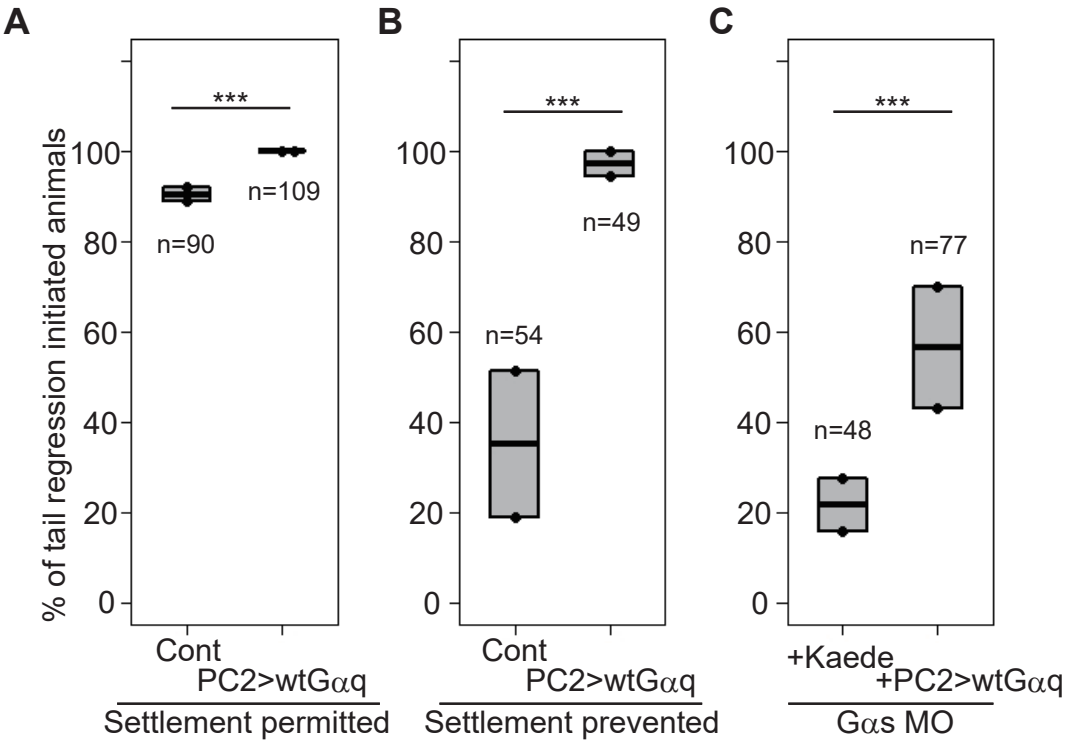

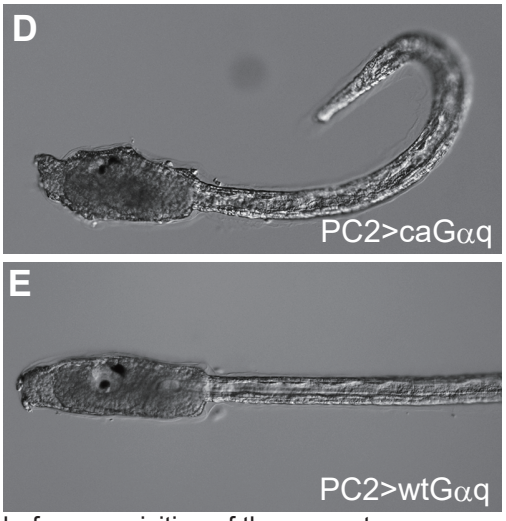

before acquisition of the competence for metamorphosis

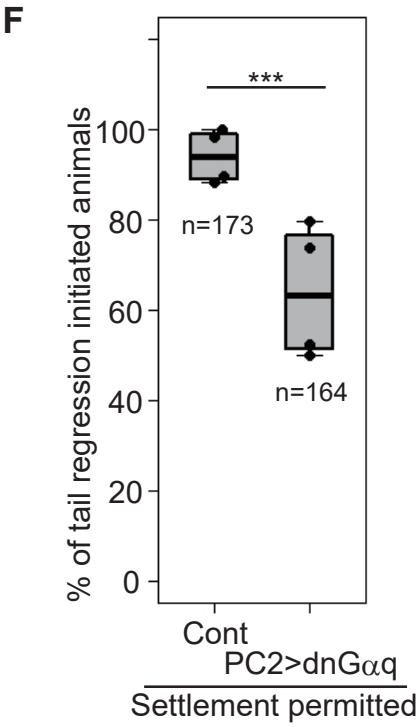

Supplementary Table S1. Expression levels of genes related to G-protein signaling during metamorphosis, as revealed by RNA-seq of the larval anterior tip including papillae

Signaling pathway	Protein name	Gene model	RPKM in sample 1	RPKM in sample 2
Gq	Gαq	KY21.Chr3.314	41.59881513	36.02858074
	IP3R	KY21.Chr8.925	8.870796516	6.554075453
	PLCβ1/2/3	KY21.Chr4.150	8.334938214	7.340493689
	PLCβ4	KY21.Chr13.136	1.822537572	1.713163972
Gs	Gαs	KY21.Chr13.220	6.051024382	7.109659594
	AC5/6	KY21.Chr14.273	4.323604525	4.916251967
	AC9	KY21.Chr14.609	13.05474647	10.4735061
	sAC	KY21.Chr10.472	0.066171013	0.035521714
	PDE1	KY21.Chr9.233	8.313399966	7.51787065
	PDE10	KY21.Chr2.501	0.01522946	0.030884959
	PDE11/5/6	KY21.Chr12.88	0.038744008	0.059477542
	PDE3	KY21.Chr14.824	4.688783832	4.554092009
	PDE4	KY21.Chr5.74	0.987514578	0.846482876
	PDE5/6	KY21.Chr1.1459	19.60592812	17.62571189
	PDE4/8	KY21.Chr5.637	3.101215703	2.859544055
	PDE9	KY21.Chr3.1286	0.116675399	0.307599189
Gi	Gαi	KY21.Chr1.1027	39.77613559	40.01167225
	dvGαi_Chr2	KY21.Chr2.875	125.3721017	134.2964969
	KY21.Chr4.943	KY21.Chr4.943	174.9101985	156.462334
GABA	GAD	KY21.Chr7.1221	3.514925048	2.987859536
	VIAAT/VGAT	KY21.Chr2.793	0.052692645	0.035619784
	GABABR1	KY21.Chr9.470	0.471066035	0.716482511
	GABABR2	KY21.Chr6.66	0.117407574	0.136471718
	GABABR2	KY21.Chr10.1059	1.816748932	0.751407557
	GIRK channel	KY21.Chr11.476	1.725547688	1.670994082
	GIRK channel	KY21.Chr13.97	3.392949104	2.96035066
Negative control[1]	VACHT	KY21.Chr1.783	0.005117048	0.025943113

1 The gene suggested not to be expressed in the papillae by *in situ* hybridization and immunostaining

Supplementary Table S2. List of candidate genes upregulated by GABA

KY21 gene model	Human homolog	[1]GABA vs Control Sample 1	[1]GABA vs Control Sample 2	[2]Papillae vs Trunk Sample 3	[2]Papillae vs Trunk Sample 4
KY21.Chr1.1223		2.33	1.97	Not determined	Not determined
KY21.Chr2.1293		2.07	3.09	Not determined	Not determined
KY21.Chr2.219		1.78	1.8	Not determined	Not determined
KY21.Chr2.1069	ASNS: asparagine synthetase (glutamine-hydrolyzing)	6.37	11.6	22.05	49.41
KY21.Chr5.240	Serine peptidase inhibitor Kunitz type 3	1.79	2.11	12.57	14.39
KY21.Chr8.1171		1.56	1.52	11.08	10.04
KY21.Chr3.438		2.38	1.91	8.61	9.16
KY21.Chr11.358		3.57	3.39	4.69	1.2
KY21.Chr9.130	CTH: cystathionine gamma-lyase	2.16	2.75	4.68	3.26
KY21.Chr9.1057	ASS1: argininosuccinate synthase 1	3.69	6.23	4.5	3.31
KY21.Chr3.1611		1.69	1.54	4.48	7.14
KY21.Chr1.732		2.34	1.66	4.37	2.74
KY21.Chr8.489	AIFM2: apoptosis-inducing factor, mitochondria-associated 2	1.85	2.05	4.01	1.77
KY21.Chr7.224	B4GALT1: beta-1,4-galactosyltransferase 1	2.43	1.51	3.99	4.16

1 The RPKM in the GABA-treated sample was divided by the RPKM in the solvent (seawater)-treated sample to calculate the scores.

2 The RPKM in the papilla region was divided by the RPKM in the remaining trunk region to calculate the scores.